

TECHNCAL UNIVERSITY OF CIVIL ENGINEERING BUCHAREST

Faculty of Building Service Engineering
Department of Thermo-Hydraulic Systems and Atmosphere Protection
CAMBI – Advanced Research Centre for Ambient Quality and Building
Physics

SUMMARY DOCTORAL THESIS

BEJAN ANDREI - STELIAN

NUMERICAL AND EXPERIMENTAL STUDY ON THE IMPLEMENTATION OF PHASE CHANGING MATERIALS IN AIR SOLAR COLLECTORS

SCIENTIFIC COORDINATOR ASSOC. PROF. CATALINA TIBERIU

BUCHAREST 2020

TABLE OF CONTENTS

Chapter 1 -	- Introdu	ction	3
Chapter 2 -	- Numeri	cal studies on the implementation of phase changing materials in solar air collectors	6
	2.1.	Introduction	6
	2.2.	Experimental setup and methodology	. 7
	2.3.	Experimental results – study of temperature variations and rise in temperature	10
	2.4.	Experimental results – analysis of heating capacity and energy produced by the solar collector	13
	2.5.	Experimental results – study of thermal transfer efficiency within the heating/charging period	14
	2.6.	Experimental results – study of the collectors efficiency within the heating/charging period	15
operatin	2.7. g hours	Experimental results – study of the solar collector coefficient of performante (COP) and number of 16	
	2.8.	Conclusions and perspectives of the experimental studies performed	18
Capitolul 3	- Modela	area numerică a colectoarelor solare cu aer cu materiale cu schimbare de fază integrate	19
	3.1.	Objectives of the numerical studies and hardware used	19
mode de	3.2. esigned	Numerical modelling of air flow through the loved holes (absorbent plate) – the first numerical 20	
material	3.3. ls – simpl	Creating the numerical model of the solar collector with lobed orifices and integrated phase chang	
	3.3.1		
	3.3.2 3.3.3		
	3.3.4	·	
	3.4.	Conclusions and perspective of the numerical studies conducted	30
Chapter 4 -	- Conclus	sions and perspectives of the current paper – personal contributions	32
Poforoncos	colocti		26

Chapter 1 – Introduction

In the current economic and energetic worldwide context it is mandatory to reduce energy consumption thus achieving a good indoor comfort. Furthermore it is imperative to reduce energy consumptions by implementing efficient solution that are using renewable energy sources and by implementing high-performance and sustainable materials. Among renewable energy sources, solar energy proves a high penetration of the Romanian and European market and also a better and better cost-benefit ratio which will determine that solar systems (both thermal and photovoltaic) to be in the future the most implemented "green" solutions worldwide. Less studied and implemented are solar air panels that have the advantage of a lower cost of implementation and the elimination of the risk of frost. Solar air collectors have received special attention in past years, as they have the potential to reduce heating consumption and preheating consumption of fresh air needed by buildings occupants. They can be implemented in the residential sector, but also in the tertiary sector, especially in industrial applications where they can maintain a minimum needed temperature or can heat the indoor air. One of the biggest challenges for the research community studying solar air collectors is the following: how to store energy and using it when solar radiation is not available? Phase change materials are materials that at certain temperatures change their phase from solid to liquid by absorbing the latent heat from the environment. When the temperature drops, the effect is reversible and the materials solidify, transferring the stored energy to the environment. Phase change materials, which store both sensible energy and latent energy, have the potential to accumulate up to 14 times more energy than classic materials.

In the current context it is very important to achieve indoor comfort with minimum energy consumption. This is only possible through the implementation of systems that use renewable energy sources and high-performance materials, as well as by correlating various active and passive strategies [1] that contributes in order to improve the building envelope, to improve thermal production methods and to improve energy storage methods. At the same time, it is important that the implemented solutions to have the lowest possible investment and operating cost so that they can be used as widely as possible and the cost-benefit ratio must be optimal.

The thermal energy storage materials (TES) are one of the most promising methods of reducing energy consumption in buildings by incorporating them into the building envelope or active systems [2]. These materials have been integrated over the time into construction materials, suspended ceilings, exterior or partition walls, ventilation systems, solar facades [3], solar collectors, photovoltaic systems, water accumulators etc. According to Heier et al. [4] materials with a role in thermal energy storage could be used for:

- reducing energy consumption by storing energy during the day and using it at night;
- reducing energy consumption by storing energy in summer and using it in winter;
- improving the efficiency of heating, cooling and ventilation systems;
- night cooling;
- improving thermal comfort by improving indoor temperature variations;
- covering the load peaks and reducing the heat demand.

Thermal mass is the ability of a material to absorb and store thermal energy [5]. In other words, in order to change the temperature of high density materials (e.g. concrete, brick, marble) a very large amount of energy is required. At the opposite, there are the materials with low thermal mass (e.g. wood, metal) which have the property of rapidly yielding the embedded heat. Materials with the role of thermal energy storage can be classified according to the type of energy stored as follows: sensible heat storage materials, latent heat storage materials and heat storage from chemical reactions [6]. Of these, phase change materials (PCM) are among the most promising because they can store 5 to 14 times more energy than conventional energy storage methods [7, 8]. According to Soares et al. [7], the implementation of phase change materials could have the following benefits:

• increasing thermal comfort by reducing the number of overheating hours, changing the surface temperature and decreasing the values of temperature peaks);

- increasing the performance of the building envelope (increasing the thermal resistance, increasing the thermal capacity);
- reducing the heating load and the cooling load by reducing the peak load and by under sizing the air conditioning systems;
- reduction of energy consumption for cooling and/or heating;
- reducing operating costs and CO₂ emissions;
- improving the efficiency of systems that use renewable energy sources.

Renewable energy sources could represent a method of energy production with a minimal impact on the environment and a low cost of implementation / operation. Of these, solar energy systems are easy to implement and can become accessible in areas with solar potential [9], with a relatively short payback period. Solar energy can be collected through solar collectors and can be transferred to water or air. Solar air collectors are a type of solar thermal collectors that use solar radiation to preheat the air introduced into a building [10]. According to Paya-Marin [10], they are usually mounted on the buildings facades, on the south side and they can have a good potential in terms of space heating, being a cost-effective solution. Solar air collectors can be classified according to their design into: glazed solar collectors, opaque solar collectors or transpired solar collectors. Solar air collectors can be used in various applications thus representing a very efficient method of capturing solar energy [11]:

- drying fruits and vegetables;
- greenhouse ventilation;
- drying of textile materials;
- keeping guard temperatures in industrial spaces;
- heating of buildings;
- preheating the fresh air needed in buildings.

According to Navarro et al. [2], thermal energy storage materials are a strategy that can improve the efficiency of systems using renewable energy sources and especially in the case of the use of solar energy. Also, thermal energy storage materials have a huge potential especially in the case of buildings with low thermal inertia and especially in the case of commercial and office buildings. Thermal energy storage materials have been used by many researchers in order to improve the efficiency of solar thermal air collectors, especially in collectors with glazed surfaces (e.g. "Trombe" type wall), but so far, very few studies are referring to the implementation of inertial elements or phase change materials in opaque transpired solar collectors [12]. The implementation of inertial materials in solar air collectors has the potential to:

- increase the number of operating hours of the system
- increase the global efficiency of the system by storing energy during the period when solar radiation is available and its emission during periods when there is no solar radiation (at night or during cloudy periods)
- improve temperature variations at the outlet of the collector
- increase the air temperature at the collectors outlet, during the period when solar radiation is not available.

Perforated solar collectors can be an affordable, efficient, cost-effective solution. They can be widely used in the industrial sector for production halls or storage halls, for maintaining a minimum temperature, for building heating or for preheating the fresh air. These collectors are already widely implemented in Canada or North Africa and are also a commercial product sold on the market. The present study aims to analyse the implementation of lobed orifices within the absorbent metal plates of the transpired solar collectors that have the potential to increase heat transfer (according to previous studies). These perforations are studied on new, large collectors, in laboratory (permanent regime), but also in real use situations (in transient regime).

The study proposes a new approach on the potential to increase the operating period and global efficiency of the air collector by implementing phase change materials that allows the accumulation of a large amount of thermal energy by storing latent energy, unlike classic materials that stores only sensible heat. In this way, the addition of inertial materials and these improved collectors can also be achieved in existing constructions without adding a lot of

weight to the structure of the building. This paper studies the implementation of phase change materials in high-performance solar collectors, both from an experimental perspective and from a numerical perspective.

The first chapter of the paper studies the current state of research in the studied field, representing an extensive bibliographic study that analyses both the implementation of phase change materials in buildings and building systems and the implementation of solar collectors in buildings, and the possibility of combining these two strategies in order to obtain a more efficient system, which allows a longer period of operation. This chapter analyses, one by one, the inertial elements that can be used for thermal energy storage systems in buildings and building systems, as well as certain types of materials for thermal energy storage, the implementation and the impact of the implementation of inertial materials in buildings and building systems. Furthermore, in the bibliographic study conducted are analysed the types of phase change materials that can be integrated in buildings and building systems, their properties, selection criteria, the phase change temperature of materials, their lifetime, and experimental and numerical methods used in the literature in order to study these systems. In the second part of the bibliographic study are analysed the solar air collectors and are highlighted, one by one: the collector types and geometries studied so far, areas of use, operating principles, operating parameters, as well as their performance and technical characteristics. According to the comprehensive bibliographic study conducted, it will be possible to notice that phase change materials have been successfully implemented in solar water collectors or opaque wall collectors, but they have not been implemented so far in solar air collectors. Also, no studies have been identified in the literature regarding the implementation of phase change materials for energy storage in transpired solar collectors used as an exterior wall in the building envelope. For this reason, it was difficult to synthesize the chapter that studies the integration of the two systems and the phase change materials and solar air collectors were exhaustive analysed.

The second chapter presents the experimental studies conducted during the doctoral studies. In order to optimize the large solar air collector, which can be implemented in real applications, several preliminary experimental studies were performed to understand the operation of phase change materials and the optimal way to position them in the air cavity. The first experimental study performed refers to the experimental analysis of the melting and solidification processes for a macroencapsulated organic phase change material integrated in a rectangular aluminium cavity. This study will analyse the possibility of integrating paraffin into rectangular metal bars and the optimal way to position them inside the air cavity of the solar collector. Then the bars will be integrated in a small solar collector previously studied in the Faculty of Building Services Engineering in order to be tested, study that will make subject to the second experimental study presented. It will establish the optimal positioning of rectangular containers and will optimize the methodology for conducting experimental studies. The third experimental study performed is represented by the analysis of the implementation of phase change materials in large solar collectors with lobed perforations (case 1 studied). The phase change materials were mounted in the middle of the air cavity of the collector thus forming a heat storage coil. Rectangular containers have spaces between them; also the metal frame on which the containers were mounted determines spaces that allow air to circulate in the sides, as well as in the lower and upper part of the collector. Irregular flow, unusual thermal stratification determined the fourth experimental study conducted, focused on the implementation of phase change materials in solar air collectors (case 2 studied). In this case, the materials are placed in the middle of the collector thus forming an obstacle that guides the airflow through the entire solar collector. This collector will prove to be the final, optimised type adopted, with differences in efficiency compared to the case 1 studied.

The third chapter presents the numerical modelling of solar air collectors with integrated phase change materials. Due to the complexity of the model, two complementary studies were performed. The first numerical study refers to the numerical modelling of the air flow through the lobed orifices of the collector and studies the impact of the lobed orifices on the air flow. The output data of this study, present the input data in the case of the second numerical study conducted which refers to the design of the simplified numerical model of the large air solar collector with lobed orifices and phase change materials. The two numerical models developed will be validated and will be the basis of the parametric studies conducted in order to optimize the solar collector prototype proposed in current paper.

Chapter 2 – Numerical studies on the implementation of phase changing materials in solar air collectors

Introduction 2.1.

This paper studies the implementation of phase change materials in perforated solar air collectors, large collectors that can be implemented in real applications. However, in order to be able to design the final collector, a series of actions and preliminary optimization studies were required. Experimental studies began by calibrating the temperature sensors used in the experimental setups. The first stage of the experimental studies is represented by the experimental analysis of the melting and solidification processes for a macroencapsulated organic phase change material integrated in a rectangular aluminium cavity. This study aims to establish the optimal solution for encapsulation of phase change materials, to establish the optimal solution for the rectangular aluminium containers position within in the collectors and to understand the phenomena that take place inside them.

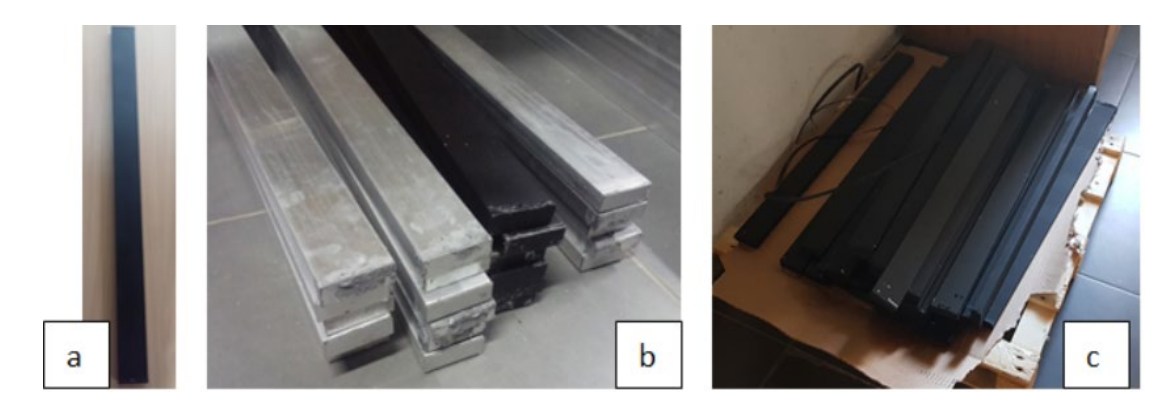


Figure 1. Containers with PCM (a - painted container with PCM; b - containers before painting; c - containers after painting)

The main conclusions of this study highlighted that newly built rectangular aluminium containers (Figure 1) with

built-in phase change materials (paraffin type RT35) are the optimal macroencapsulation solution, occupying all	the
space available and that the vertical positioning inside the collector is the optimal one, due to the enhanced h	ıeat
transfer. The properties of the phase change material used are presented in Table 1 and Figure 2, the melt	ing
temperature being chosen according to the studied literature, around 35 °C. Each aluminium bar (800x60x20m	ım)
contains 0.7l PCM when it is in liquid state, respectively 0.54kg PCM.	

Property	Value	Unit
Melting interval	29-36	°C
Solidifying interval	36-31	°C
Heat stores are site (2) (419C) +7.59/	160	kJ/kg
Heat storage capacity (26-41°C) ±7,5%	45	Wh/kg
Specific heat	2	kJ/kgK
Solid density (la 15°C)	0.86	kg/l
Liquid density (la 45°C)	0.77	kg/l
Thermal conductivity	0.2	W/mK
Volume variation	12.5	%
Maximum operation temperature	65	°C
Lifetime	unlimited	-

Table 1. Properties of the phase change materials used - RT35 [13]

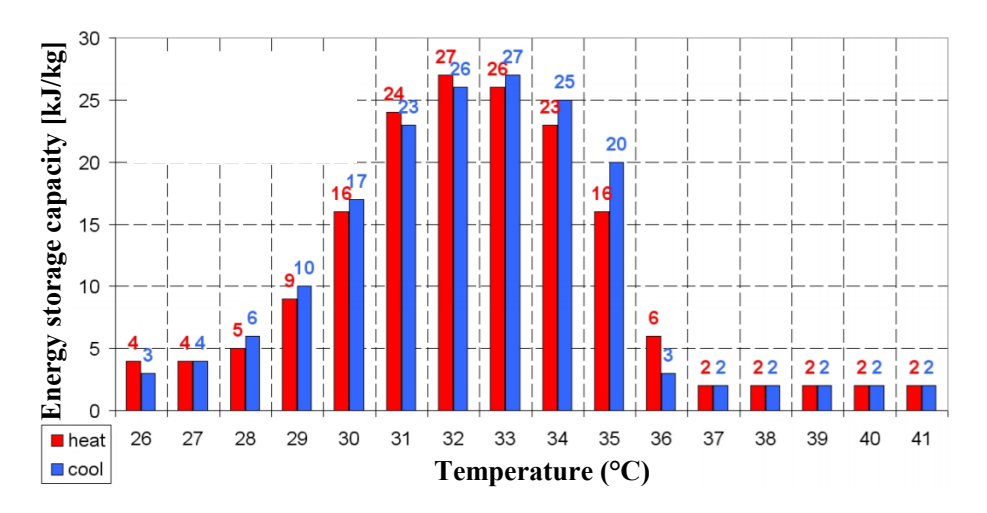


Figure 2. Energy storage capacity for the organic PCM (RT35 – paraffin) [13]

The second stage of the experimental studies conducted is the testing of the rectangular containers with PCM within small dimensions perforated solar collectors previously studied within the Faculty of Building Services Engineering and their positioning on the back wall of the collector. This preliminary study aims to identify the optimal position of the PCM bars inside the air cavity and to test the possibility of implementation in larger, real-scale air solar collectors. The results of this study showed that the implementation of phase change materials has the potential to increase the number of operating hours of the collector, by accumulating energy during the period when solar radiation is available. This study also showed that longer periods of time are needed for experimental studies and that it is necessary to place the PCM coil in the centre of the air cavity in order to increase heat transfer.

After testing the containers placed within the small-size air collectors, the study of the implementation of phase change materials in the large-scale collectors follows, in the situation when they are placed on a metal frame in the middle of the air cavity, thus creating a thermal energy storage coil (case 1, the first design studied). In this case, the rectangular aluminium bars have spaces between them that favour the heat transfer. Moreover, the metal frame on which they are placed, forms spaces that favour the airflow trajectory, but also determines a thermal stratification and a pressure distribution due to the location of the fan at the top of the collector.

The results of this preliminary study showed that the positioning of phase change materials in this case (heating coil/battery), in which rectangular aluminium bars have spaces between them, is not an optimal positioning due to the thermal stratification inside the cavity and vertical pressure differences. The positioning of the PCM bars causes pressure losses that favour a deficient heat transfer, also caused by the location of the fan at the top of the collector. This study led to the fourth stage of experimental studies the analyses the large-scale solar collector with phase change materials integrated in rectangular aluminium containers that forms an obstacle inside the air cavity, forcing a guided airflow inside it. This is the final, optimized transpired air solar collector that is the subject of this paper and on the basis of which numerical studies were performed, and its construction, experimental stand, measurement protocol and results are presented below.

2.2. Experimental setup and methodology

Figure 3 shows the geometry of solar collectors built with their dimensions and components. The solar collector is made of an absorbent metal plate with lobed perforations through which the outside air is aspired into a rectangular cavity with walls made of several layers, respectively: OSB inside, thermal insulation (4cm) and OSB outside. The air gap thus created inside the collector has the following dimensions: $2000 \times 1020 \times 280$ mm. The air collected in the interior air cavity goes than at the upper part of the collector and is sucked through a gap with dimensions of 830×150 mm. Afterwards, it is introduced into a thermal insulated mixing box, from where it is further evacuated by using an Ebmpapst variable speed fan (through a hole with a diameter of 180mm). A mobile metal frame was mounted inside the solar collector, representing the support of the rectangular aluminium containers with embedded phase change materials. This frame will be used in order to study the optimal positioning of the inertial materials inside the cavity.

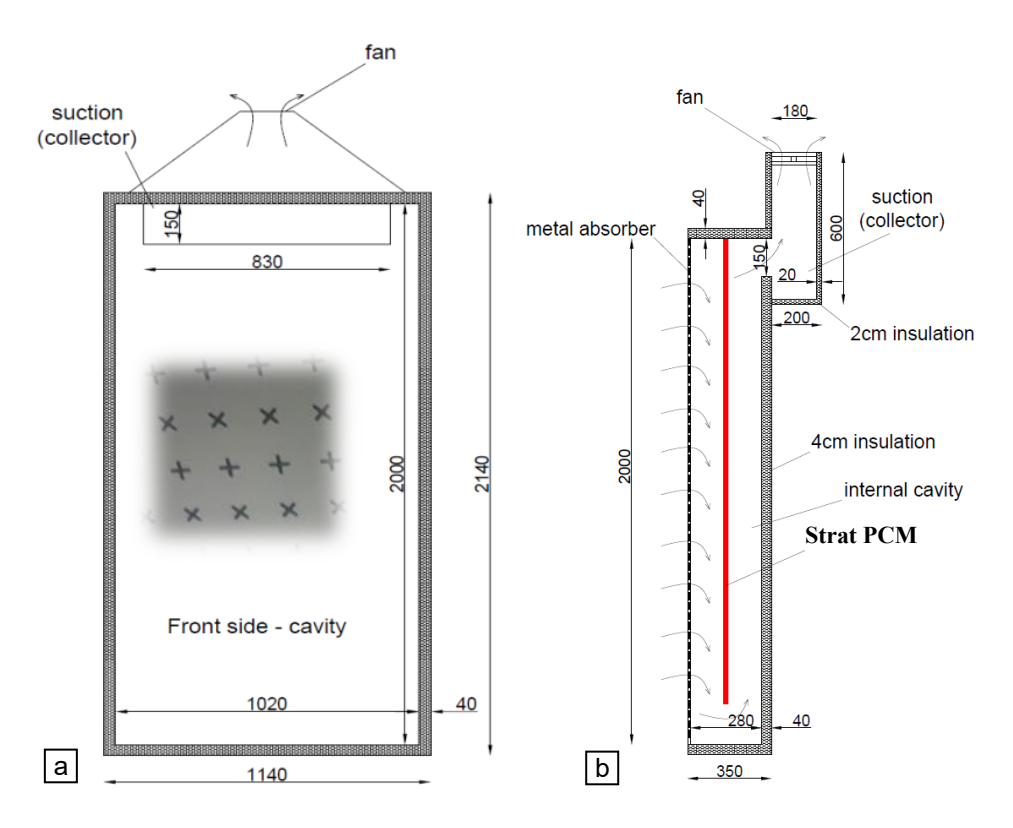


Figure 3. Geometry of the new proposed, final solar collector, with the PCM layer forming an obstacle - case 2: longitudinal section (a) and cross-section in which the PCM obstacle can be observed (b)

After the air runs through the lobed orifices and the heat is transferred from the absorbent plate, the air enters the interior cavity and follows a downward trajectory due to the phase change material obstacle. The obstacle consists of rectangular aluminium containers glued together with macroencapsulated RT35 phase change materials integrated. The bars used in the previous study were glued together and the spaces were filled with extruded polystyrene, keeping the same conditions as in the previous case, as well as the same amount of phase change materials. The geometry of the lobed holes is shown in Figure 3a. The pitch between the holes is 20mm (between axes), on each plate there are approximately 5000 lobed holes (100x50), being placed alternately: '+', 'x', '+', 'x' etc. Both types of orifices, both the lobed and the circular ones, have the same surface (19.635mm²) and the same equivalent diameter of 5mm. Figure 4 shows the air solar collector with lobed holes and in the middle of the cavity it can be observed the mobile frame with PCM that determines an obstacle for the airflow.



Figure 4.Experimental setup – transpired solar collectors (permanent regime) – geometry of the solar collector

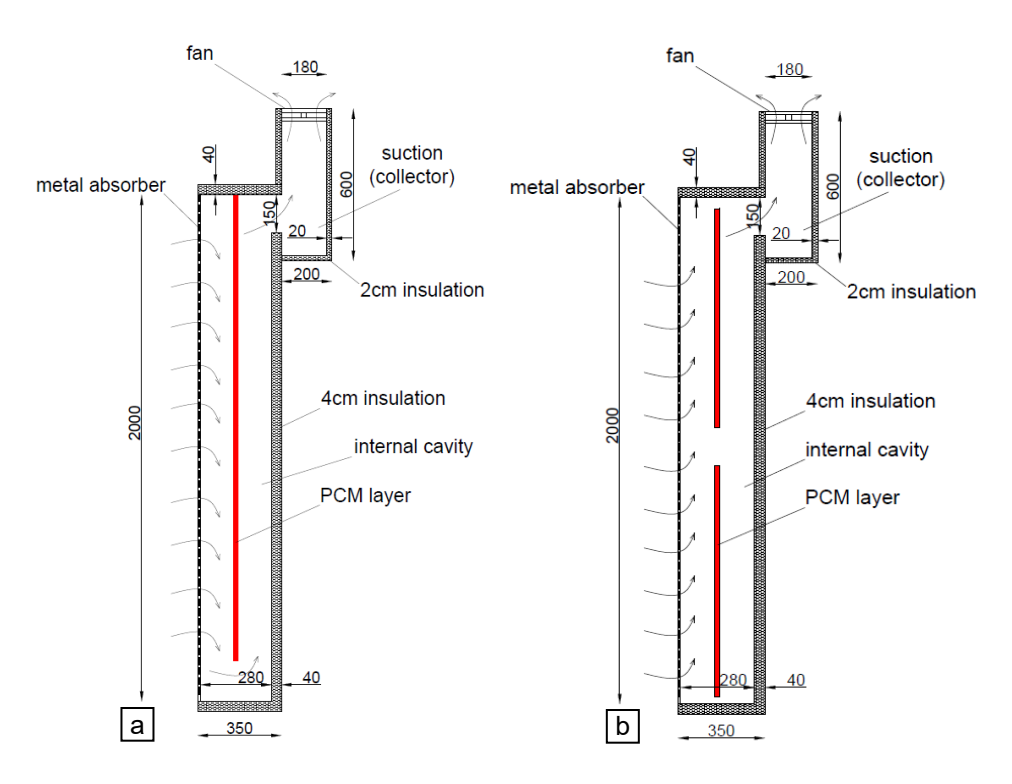


Figure 5. Cross section with the position of phase change materials inside the large-scale final solar collector - case 2 (a) vs. first solar collector studied - case 1 (b)

Figure 5 and Figure 6 highlights the differences between the previous case (case 1) in which the aluminium bars with embedded PCM were positioned on the mobile frames of the collector in the middle of the air cavity, forming two areas (coil/battery storage), but also some spaces that favoured an uneven distribution of air flow and unfavourable thermal stratification. The new solar collector (Figure 5b and Figure 6b) features a continuous phase change material layer (obstacle) that guides the air flow, ensuring the 'washing' of the entire heat exchange surface between the air and the PCM, as well as a superior heat transfer.

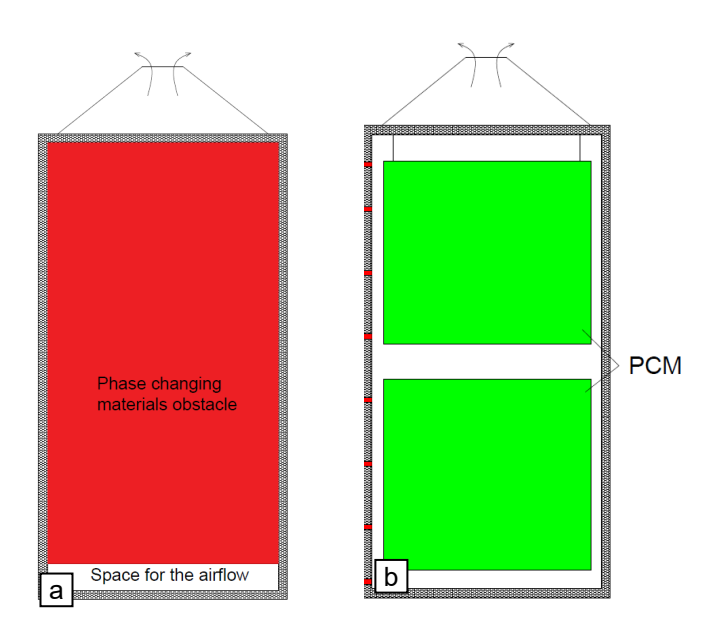


Figure 6. Longitudinal section with the position of phase change materials inside the large-scale final solar collector - case 2 (a) vs. first solar collector studied - case 1 (b)

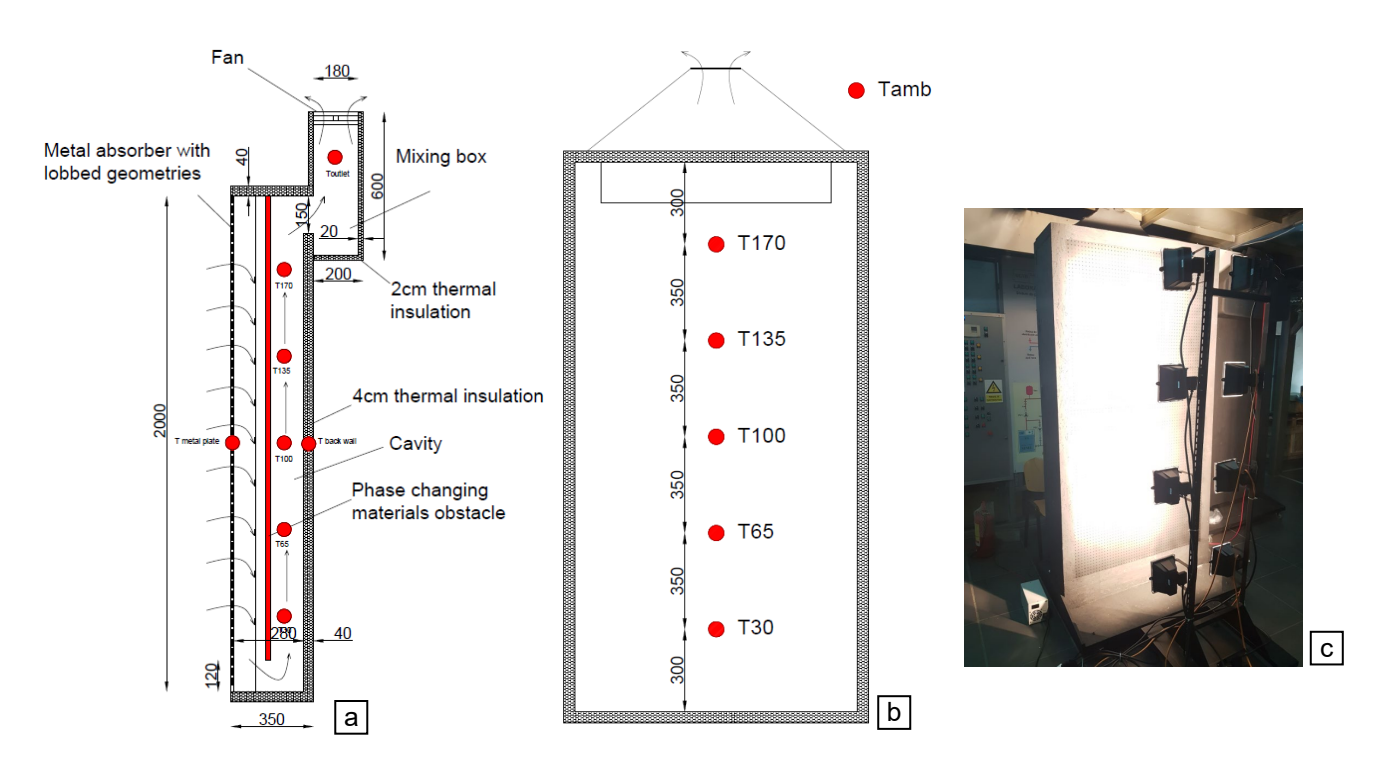


Figure 7. Experimental setup layout – position of temperature sensors inside the new solar collector studied – case 2; a – cross-section, b – longitudinal section, c – actual experimental setup during studies

In order to measure temperature values in different point of the solar collectors, 9 sensors were used (thermistors K-type, ± 0.2 °C) and their positioning is highlighted in Figure 7:

- one sensor for measuring temperatures on the absorbent metal plate (Tmetal plate)
- one sensor for measuring the temperature on the back wall of the collector (Tback wall)
- five sensors that measure the thermal stratification within the air cavity (T30, T65, T100, T135 and T170) located in the second newly formed air cavity
- one sensor for measuring the temperature of the exhaust air (Toutlet)
- one sensor for measuring ambient temperature (Tamb).

Moreover, for the numerical studies that are the subject of the next chapter, two temperature sensors were installed that measure the air temperature at 5 cm distance from the absorbent plate, in the first air cavity and a sensor that measures the temperature on the surface of the bars (measuring the material temperature). The measurements were performed at a time interval of one minute and the data were recorded using an ALMEMO 710 data logger. In order to reproduce solar radiation, eight 500W halogen projectors were used and positioned at 0.8m distance from the absorbent plate for a uniform temperature distribution (according to the literature they will simulate a solar radiation of approximately 800W /m²). The airflow circulated by the Ebmpapst fan supplied from the RXN-602D DC source is 400m³/h, respectively 200m³/h/m² of collector. The measurements were performed for 1200 minutes (20 hours). The lamps were switched on in the 25th minute in order to simulate the solar radiation, respectively the heating / charging stage of the phase change materials and were switched off after approximately 370 minutes (in the 395th minute) to simulate the cooling / discharge period of the phase change materials, when solar radiation is no longer available. The discharge period lasts for 805 minutes, up to the 1200 minute when the measurements were stopped. As in the previous case, 28 rectangular aluminium bars are placed inside the solar collector totalling about 19.6l PCM when the material is in the liquid phase, respectively about 15.1kg PCM.

2.3. Experimental results – study of temperature variations and rise in temperature

Following the experimental studies conducted, some very interesting aspects could be found. Figure 8 shows the temperature variations for five points for the case of the collector with lobed holes, without PCM: outlet temperature (Toutlet), temperature in the middle of the collector (T 100 middle), temperature of the rear wall of the

collector (T back wall), the absorbent plate temperature (T metal plate) and the ambient air temperature (T ambient). At an ambient temperature of 24.5°C (minute 390), the exhaust air temperature is 34.7°C, resulting in a rise in temperature of 10.2°C. The temperature difference thus obtained in case 2 (with obstacle) is 9.7% higher than in case 1 in which the PCM layer is in the form of a storage battery.

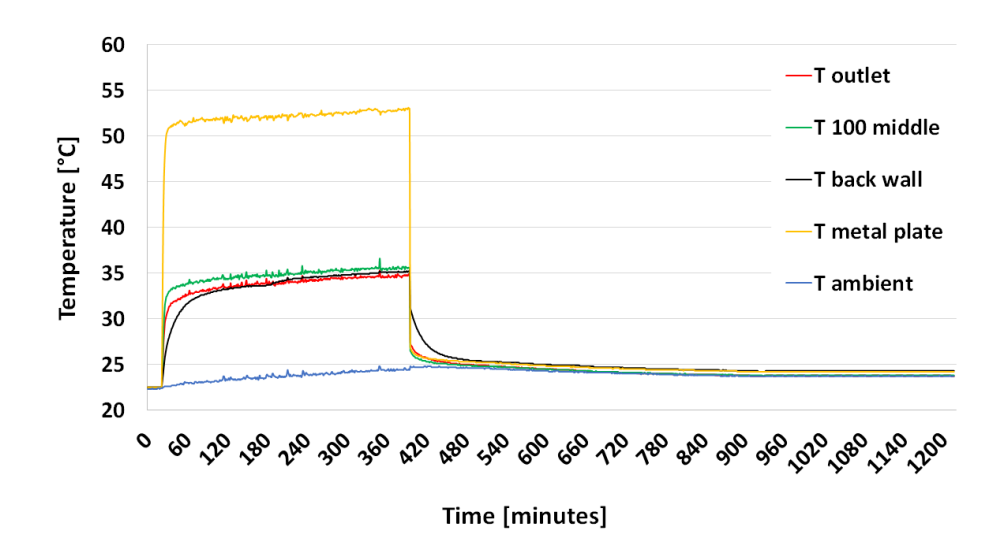


Figure 8. Solar collector with lobed orifices without PCM, temperature values obtained in 5 reference points – case 2

It can be observed that the temperature at the outlet of the collector has values close to the air temperature in the middle and the temperature of the back wall of the collector, which may be due to heat transfer that occurs mainly in the first air cavity formed between the absorbent plate and obstacle. After turning off the lamps, the values of the five measured temperatures equalize quickly, only the temperature of the back wall has a phase shift of about 140 minutes, constituting a small thermal mass.

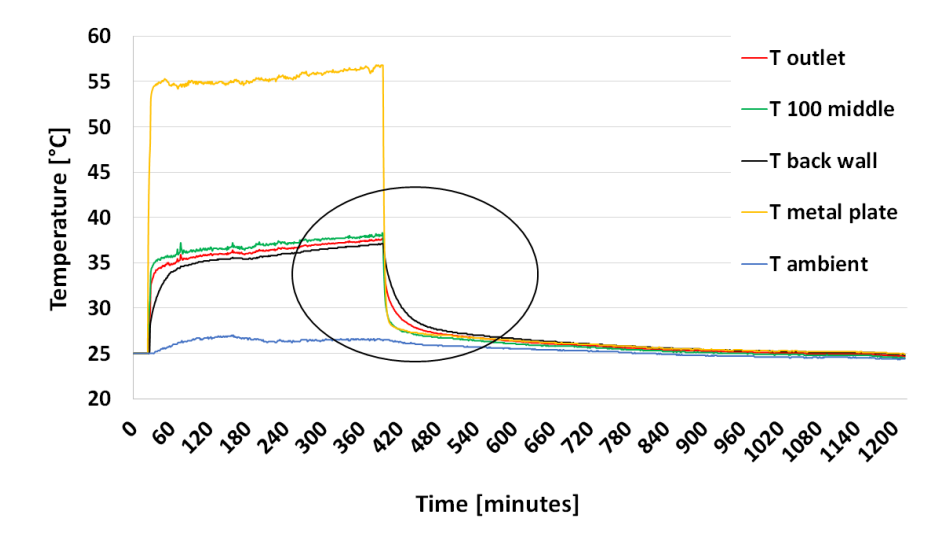


Figure 9. Solar collector with lobed orifices with PCM, temperature values obtained in 5 reference points – case 2

In Figure 9 we can observe that the temperature variations for the same five points, for the case of the solar collector with lobed orifices and with the PCM layer forming an obstacle inside the cavity. At an ambient temperature of 26.5°C (minute 390), the exhaust air temperature reaches 37.6°C, resulting a rise in temperature of 11.1°C. The temperature difference thus obtained in case 2 (with PCM obstacle) is 7.8% higher than in case 1 (with

PCM layer forming a storage battery/coil). At the same time, the temperature measured on the metal absorbent plate is 56.8°C, the temperature on the back wall is 37.1°C and the temperature in the middle of the collector is 38°C. It can be noticed that the temperature on the collectors outlet has values lower than the temperature in the middle of the cavity especially in the first time period of the measurements, when the phase change materials from the top of the collector are storing latent energy, but later on, the two values gradually equalize. After the projectors are switched off, the energy is slowly released to the air circulating inside the collector. Unlike case 1, part of the energy stored in the PCM is transferred to the absorbent metal plate due to the circulation of air through the first air cavity formed. Furthermore, some of the energy accumulated by the PCM is transferred to the back wall. Moreover, the energy accumulated during the period when the solar radiation is available is slowly yielded to the airflow circulated through the transpired collector when the solar radiation is not available.

Furthermore, maybe the most important parameter in the case of the study of a solar air collector is the analysis of the rise in temperature variation determined by the use of the transpired collector with and without embedded PCM. Figure 10 emphasise the variation of the temperature difference between the air exhausted from the collector (Toutlet) and the ambient air (rise in temperature), in both cases, with and without integrated PCM. The impact of phase change materials is very clear, by accumulating the energy during the heating period in which solar radiation is available and by the yield of energy during the cooling period in which halogen lamps are switched off. It can be observed that in the case of the solar collector without PCM the variation is relatively linear starting with 80th minute and reaches a maximum of 10.2°C (higher than in case 1, previously studied). On the other hand, in the case of the solar collector with PCM, if at the beginning this variation has lower values than in the case without PCM (interval 60-240 min.), due to melting of PCMs and because of the energy stored within PCMs, after the 240th minute, the rise in temperature is higher and reaches a maximum of 11.1°C, respectively 8.8% more than the case without PCM (higher value than in the case 1 studied previously). The melting phenomenon of the PCMs is obvious for 180 minutes. Moreover, the solar collector with the PCM obstacle has a higher rise in temperature than in the case 1 of the solar collector with two PCM zones and spaces between the aluminum bars, in both situations: with (7.8%) and without PCM (9.7%). After the solar radiation is stopped, the temperature of the exhaust air from the solar collector in the case without PCM quickly reaches the ambient air temperature (after about 70 minutes), while in the case of the collector with PCM, the exhaust air temperature is higher for 800 minutes, until the temperatures equalize at the end of the measurements. After switching off the lamps, the temperature of the exhaust air from the collector with PCM is higher than the ambient air temperature by up to 1.1°C, reaching higher values even by 2.4°C (especially at the beginning of the cooling/discharge process). It can be seen that the energy stored by phase change materials is released more slowly in the case of the collector with obstacle than in the previous case, due to the reduction of heat exchange surface and due to the fact that heat exchange will occur mainly in the first air cavity.

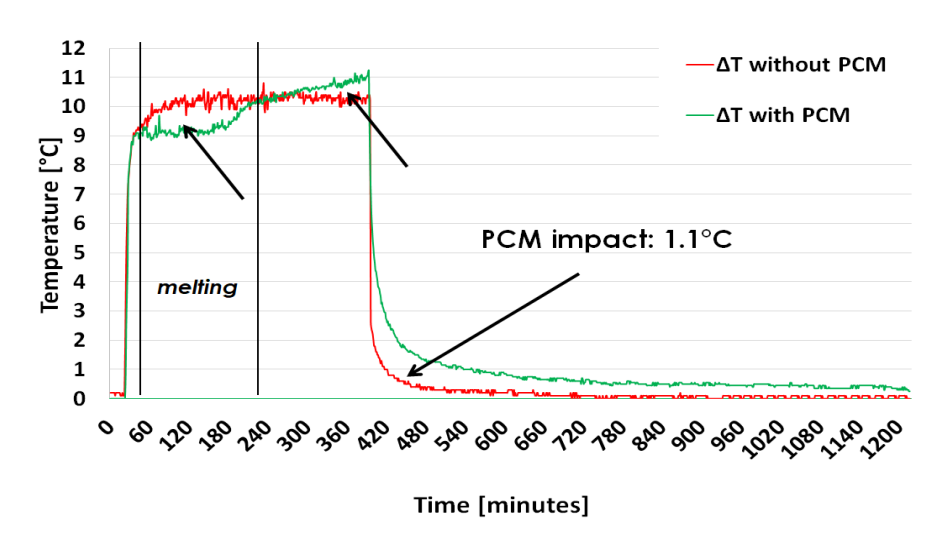


Figure 10. Rise in temperature – case 2 (Toutlet – T ambient)

2.4. Experimental results – analysis of heating capacity and energy produced by the solar collector

In this subchapter, the variation of the heating capacity of the two solar collectors and of the thermal energy produced by them will be analysed. The heating capacity Q [W] and the thermal energy produced by the solar collector E [Wh] can be calculated using the following formulas:

$$Q = D \bullet \rho \bullet c_p \bullet \Delta T [W]$$

$$\Delta T = T_{outlet} - T_{ambient} [°C]$$

$$E = Q \bullet t [Wh]$$

, were:

D = airflow through the solar collector [m³/h]

 $\rho = air density = 1.2 kg/m^3$

 $c_p = air specific heat = 1.013 kJ/kg^{\circ}C$

 ΔT = rise in temperature = temperature difference between air exhausted from the solar collector (T_{outlet}) and ambient air ($T_{ambient}$)

t = time period [s].

Figure 11 shows the variation of the heating capacity for both solar collectors during the experimental measurements. The maximum heating capacity of the solar collector without PCM is 1458.7W (324^{th} minute), respectively 1.46kW, while the solar collector with PCM reaches a maximum of 1519.5W (394^{th} minute), respectively 1.52kW, with 4.1% more. As it can be observed, the peak capacity is reached faster in the case of the collector without PCM due to the lack of thermal inertia. The maximum specific power of the solar collector without PCM is $729.4~W/m^2$ ($0.73kW/m^2$), while in the case of the collector with PCM, it reaches a slightly higher value, respectively $759.8~W/m^2$ (0.76kW) / m^2 .

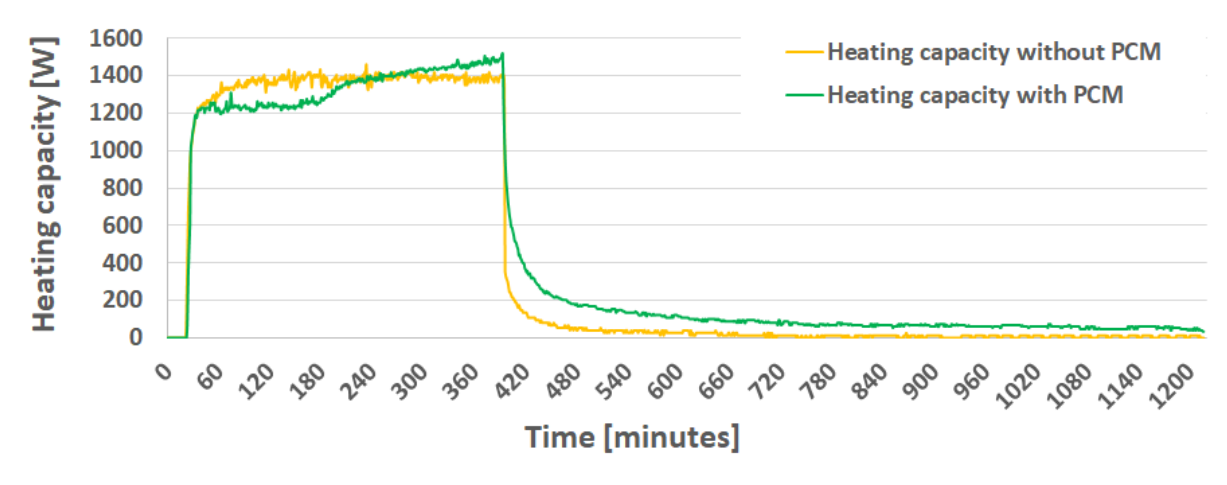


Figure 11. Heating capacity variation of the solar collectors with and without PCMs

The specific heating capacity (Q_{spec}) of each solar collector can be calculated with the following equation:

$$Q_{spec} = Q/S [W/m^2]$$

, where:

Q = heating capacity of the solar collector [W]

S = absorbent plate surface [m²].

During the heating / charging period, the average heating capacity of the solar collector with PCM is 1.32kW ($0.66kW / m^2$), slightly lower than the in the case of the solar collector without PCM which reaches a value of

1.36kW (0.68kW / m²), which it is due to the energy stored in the PCMs. During the cooling / discharge period, the average heating capacity of the solar collector with PCM is 117W (58.5W / m²), almost 4.7 times higher than the solar collector without PCM which reaches a value of 25W (12.5W / m²), due to the energy transferred from the phase change materials to the air flow through the solar collector. It can also be noticed that during the heating / charging period the energy is stored faster (melting process is more clear between 60th minute and 240th minute), while the solidification process occurs more slowly, during the whole cooling / discharge stage, with a period in which the process is more intense (between 400th minute and 660th minute).

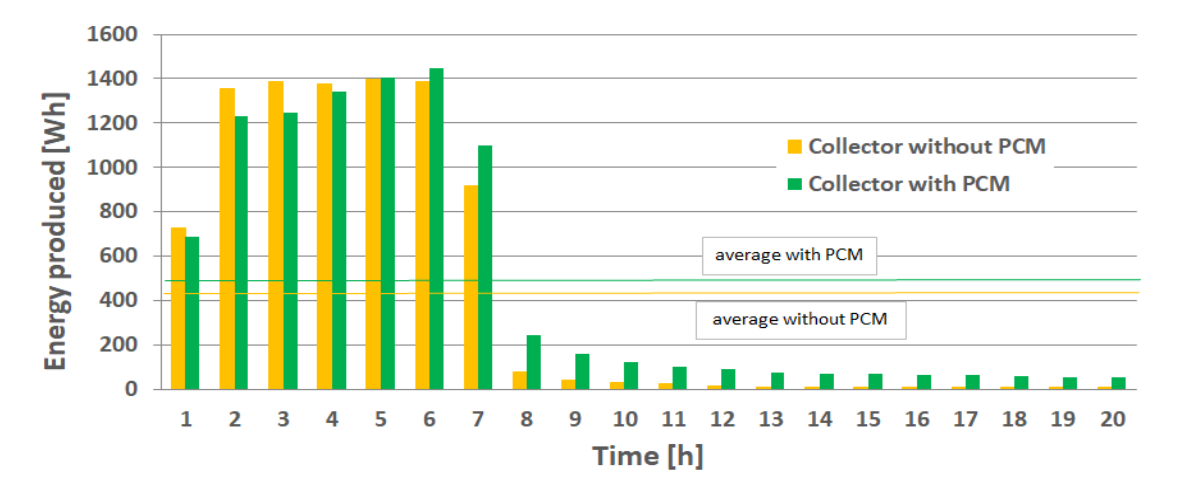


Figure 12. Energy produced each hour by the collectors with and without PCMs

Figure 12 shows the amount of thermal energy produced by the two solar collectors with and without PCM in each hour of operation during the experimental measurements. It can be seen that when using PCM the solar collector produces a maximum of 1.445kWh in one hour of operation (6th hour), while the collector without PCM produces a maximum of 1.397kWh (5th hour). The solar collector with PCM produces an average of 484Wh per hour of operation during experimental studies, while the solar collector without PCM produces an average of 440Wh. During the heating / charging period the amount of energy produced by the solar collector is similar in both cases, the differences appearing in the first part of the experimental studies when the phase change materials change their state of aggregation. In contrast, during the cooling / discharging period, the amount of energy produced by the solar collector with PCM is up to 9 times higher in certain hours. In the heating stage the solar collector with PCM produces 7.4kWh, less than the solar collector without PCM which produces 7.6kWh. In the cooling stage the solar collector with PCM produces 2.3kWh, twice as much as the solar collector without PCM which produces 1.2kWh. By comparing the two collectors with and without PCM during the whole period of experimental studies, the total amount of energy produced by the collector without PCM is 8.8kWh (4.4kWh / m²), while the solar collector with PCM produces 9.7kWh (4.85 kWh / m²), respectively with 10.2% more energy in the 20 hours of operation. This can be explained by the fact that rectangular bars with embedded phase change materials captures more energy from the solar radiation that enters through the lobe holes of the absorbent metal plate, thus improving heat transfer. The specific energy produced (E_{spec}) by each solar collector can be calculated with the following equation:

$$E_{spec} = E/S [Wh/m^2]$$

2.5. Experimental results – study of thermal transfer efficiency within the heating/charging period

According to the literature, in addition to the rise in temperature analysis and to the heating capacity variation study, it is important to analyse the efficiency of heat transfer during the heating period (ε) , when solar radiation is available (lamps are on). The heat transfer efficiency can be calculated as the ratio between the collectors rise in temperature and the difference between the average temperature on the absorbent metal plate and the ambient temperature and can be calculated with the following equation:

$$\varepsilon = (T_{\text{outlet}} - T_{\text{ambient}}) / (T_{\text{metal plate}} - T_{\text{ambient}}) [\%]$$

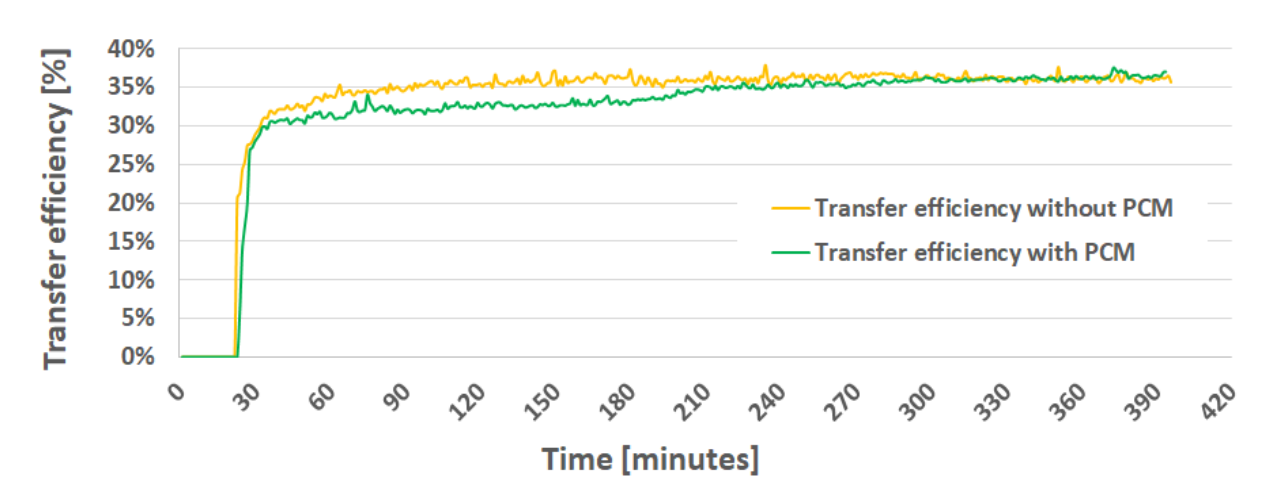


Figure 13. Heat transfer efficiency with and without PCM

The variation of the heat transfer efficiency for the two collectors is presented in Figure 13. It can be observed that the heat transfer efficiency in the case of the solar collector with PCM has constantly lower values than in the case of the collector without PCM. The average transfer efficiency for the collector with PCM is 34.11%, while the average collector efficiency in the case without PCM is 35.6%. This may be due to the fact that part of the energy absorbed by the absorbent metal plate is yielded by radiation to the obstacle with integrated phase change materials, heat transfer efficiency taking into account only the temperature of the perforated plate lobed. This phenomenon is especially visible in the first part of the heating / charging stage between the 30th minute and the 210th minute in which the PCM melting occurs. After this minute, the transfer efficiency is equalized, the solar collector with PCM reaching the maximum value of 37.54%, while the solar collector without PCM reaches the maximum value of 37.89%. During the cooling / discharge period, the efficiency of the heat transfer cannot be evaluated as the temperature of the absorbent plate is relatively equal to the ambient air temperature. The overall efficiency of the collector can be estimated by analysing the coefficient of performance of the solar collector (COP).

2.6. Experimental results – study of the collectors efficiency within the heating/charging period

According to the studied literature, beside the analysis of the rise in temperature of the collector, the analysis of its heating capacity, the analysis of the energy produced by it and the analysis of the heat transfer efficiency during the heating period, another important factor that must be studied is the collector efficiency (η) . The efficiency of a solar collector depends on its heating capacity (Q, previously calculated), the surface of the absorbent plate (S) and the incident solar radiation on the metal plate and can be calculated with the following equation:

$$\eta = P / Q \cdot I_r [\%]$$

, where:

 $I_r = \text{solar radiation } [W/m^2].$

Figure 14 shows the variation of the solar collectors' efficiency with and without integrated phase change materials. The variation is similar to the variation of the rise in temperature, as all other terms involved have constant values: airflow, specific heat, density, exchange surface or solar radiation. It can be observed that the efficiency of the solar collector with PCM is lower in the first part of the heating / charging process due to the accumulation of latent heat in the phase change material and after the melting of the material, its efficiency is higher due to improved heat transfer (PCM layer captures solar radiation through the lobed orifices of the absorbent metal plate and stores sensible heat when it is in the liquid phase). The maximum efficiency of the collector with PCM is 94.97%, while the maximum efficiency of the collector without PCM is 91.17%. However, the average efficiency of the solar collector with PCM is lower during the heating / charging period due to the phase-changing materials that accumulate energy: 83.59%, as opposed to 85.54% in the case without PCM. According to the studied literature, halogen lamps placed according to the experimental setup presented above can generate the equivalent of a solar

radiation value of 800W / m². However, this value is estimated and the study of the solar collector efficiency will be further studied. During the cooling / discharging period, the efficiency of the solar collector cannot be evaluated as the halogen lamps are switched off, thus simulating the period when the solar radiation is not available. The overall efficiency of the collector can be properly estimated by analysing the coefficient of performance of the solar collector (COP).

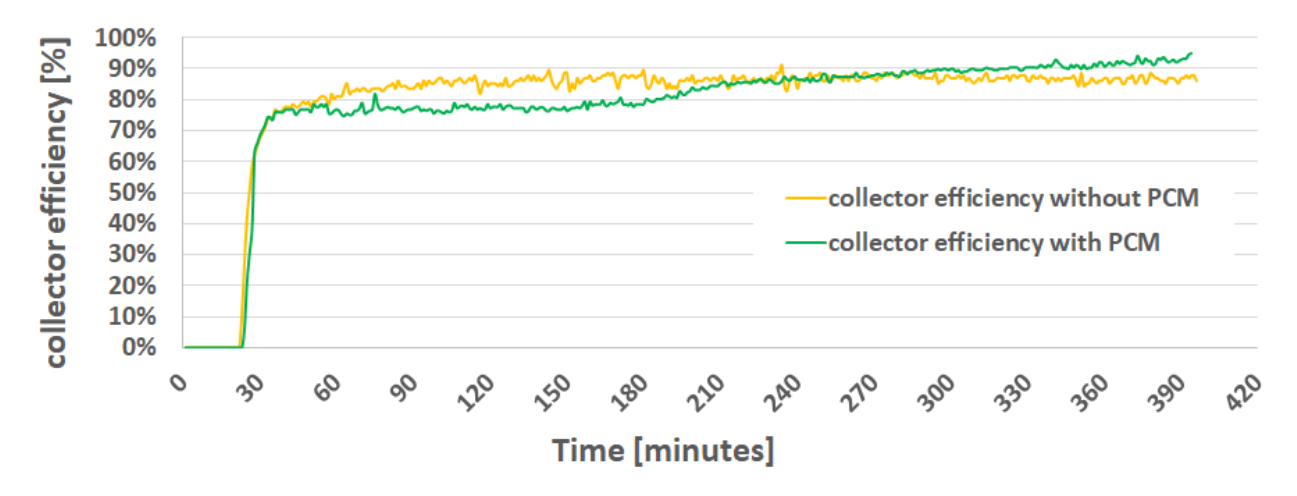


Figure 14. Solar collector efficiency with and without PCM

2.7. Experimental results – study of the solar collector coefficient of performante (COP) and number of operating hours

As the overall heat transfer efficiency and the overall efficiency of the solar collectors cannot be evaluated for the whole studied period, including the cooling / discharge stage, because the value of solar radiation is zero and the absorbent plate temperature is relatively equal to the ambient air temperature, it is necessary to introduce a new parameter in order to assess the global efficiency of the two solar collectors.

Poole et al. [14] mentions in his paper the term "solar collector coefficient" (COP) calculated similarly as for heat pumps, as a ratio between the thermal energy produced by the solar collector (E) and the electricity consumed by the fan used for air circulation (E_{vent}) or as a ratio between the heating capacity of the solar collector and the electric power of the fan ($P_{vent} = 67W$). The formula for calculating the coefficient of performance of the solar collector is presented below:

$$COP = E/E_{vent} = P/P_{vent}$$

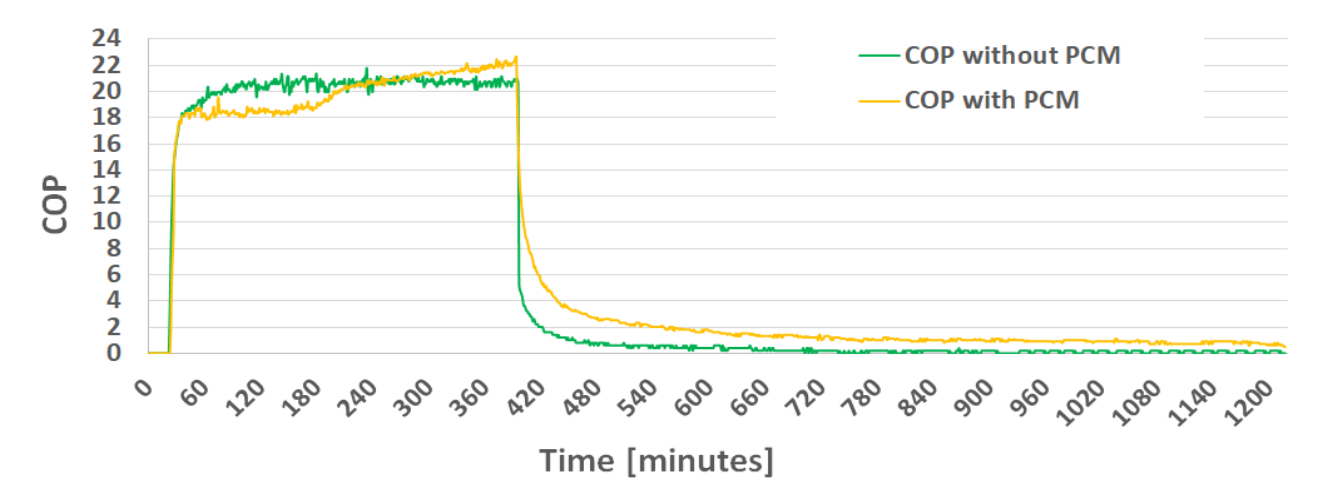


Figure 15. COP variation for the solar collectors with and without PCM

Figure 15 shows the variation of the COP for the two solar collectors with and without PCM, the variation of these values being similar to the variation of the collectors rise in temperature. The maximum COP in the case of the solar collector with PCM is 22.7, while the maximum COP of the collector without PCM is 21.77. Due to the presence of phase change materials, during the heating / charging period, the collector with PCM has a significantly lower average COP than the solar collector without PCM: 19.7, compared to 20.3. Obviously, during the cooling / discharge period, the collector with PCM has an average COP even four times higher than the solar collector without PCM: 1.7, compared to 0.4. When the COP value of the solar collector falls below 1, heating with an electric battery becomes more economically advantageous. Therefore, from 457th minute, the solar collector without PCM should be turned off, while the solar collector with PCM should be turned off from 937th minute, when the COP reaches a value bellow 1, although it can still provide thermal energy (about 0.3kWh more).

Figure 16 highlights the average value of the COP in each hour of operation. It can be seen that the COP of the solar collector with PCM is lower in the first stage of the study, because the phase change materials stores energy, while after stopping solar radiation, the COP is considerably higher in case of the collector with integrated PCM.

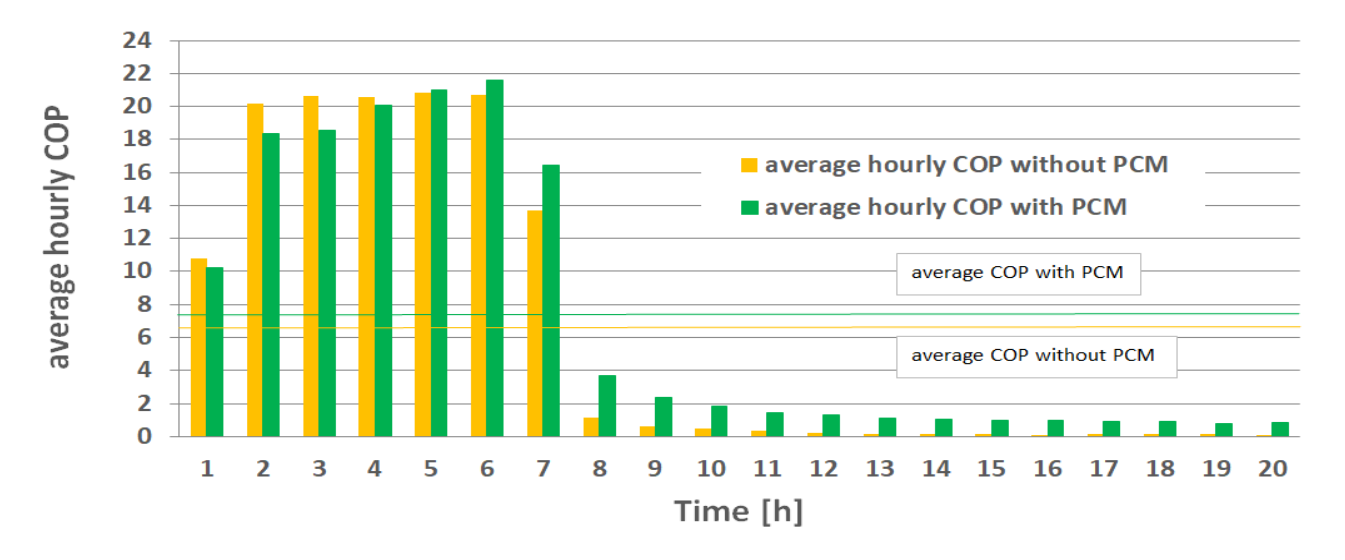


Figure 16. Average hourly COP of the solar collectors with and without PCM

The average COP of the solar collector without embedded phase change materials is 6.6, while the average COP of the solar collector with embedded phase change materials is 7.3, respectively 10.6% higher. Therefore, we can conclude that the overall efficiency of the solar collector is 10.6% higher in the case of the PCM collector.

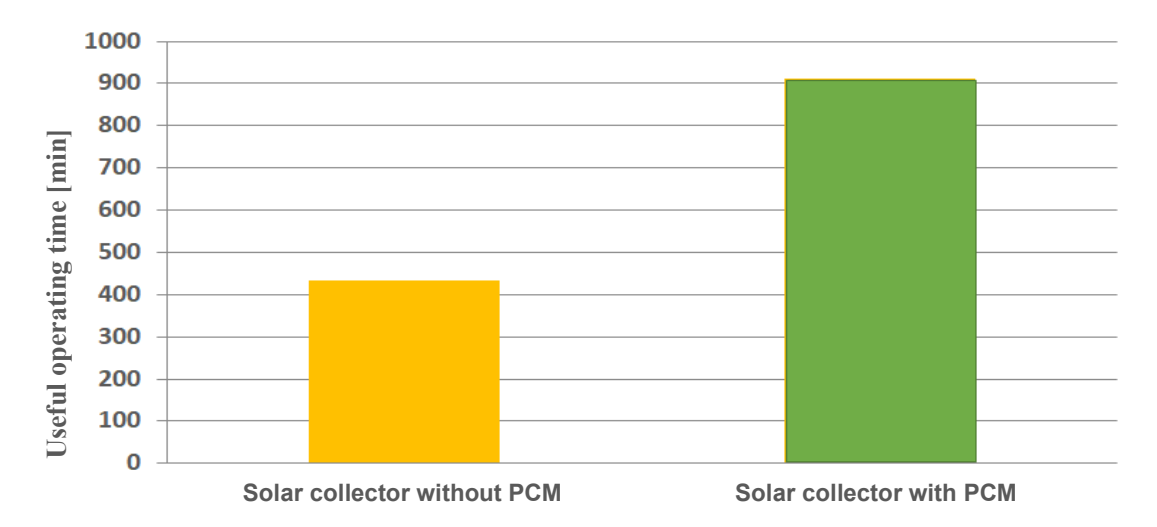


Figure 17. Useful operating time of the collectors with and without PCM

During the heating / charging period the energy is stored faster (melting process is very clear between 60th minute and 240th minute), while the solidification process occurs more slowly, during the whole cooling / discharging

stage, with a certain period in which the process is more obvious (between 400th minute and 660th minute). Therefore, the heating/charging process occurs quickly being supported by solar radiation, while the cooling/discharge process is slow and requires new methods useful in order to improve heat transfer.

The useful operating time of the solar collectors can be defined as the time interval in which the coefficient of performance of the collector is above 1, being more efficient than conventional electric heating. Figure 17 shows the useful operating time period for the two solar collectors. In the case of the solar collector without PCM, the COP has a value above 1 from 23rd minute to 457th minute, resulting in 434 minutes of operation. Unlike the classic collector, the solar collector with PCM has a COP value above 1 starting with 23rd minute and up to 937th minute, resulting in 913 minutes of operation. Analysing these aspects we can conclude that in case of using PCM, the solar collector has a useful period of operation 110% longer than the collector without PCM, respectively it works 480 minutes longer, in the same time period studied.

We concluded, therefore, that conducting the study in permanent regime, the transpired solar collector with integrated phase change materials has the potential to increase the overall efficiency of the system, to increase the number of operating hours and the temperature difference between the ambient air and the exhausted air (rise in temperature). In order to analyse the improvement of temperature variations and to analyse the real impact of the collectors, it is necessary to study the collectors in a transient regime.

2.8. Conclusions and perspectives of the experimental studies performed

After studying the aluminium containers with macroencapsulated phase change materials, conducting the preliminary study in small collectors and performing the first study on large collectors in which the PCM layer formed a coil in the middle of the air cavity, we decided to improve the collector, resulting in its final design on which this paper is focusing and on which the following numerical studies were conducted. This chapter studies the implementation of phase change materials in a obstacle that guides the air flow inside the solar collector. After several experimental studied conducted, the following could be concluded:

- the rise in temperature in case of the collector without PCM is maximum 10.2 °C (9.7% more than in the case of the collector without the interior obstacle)
- the maximum temperature of the air exhausted from the solar collector without PCM is 34.7°C
- the rise in temperature for the collector with PCM reaches a maximum of 11.1 °C (7.8% more than in the case of the collector without the interior obstacle)
- the maximum temperature of the air exhausted from the solar collector with PCM is 37.6 °C
- the rise in temperature is higher in the case of using PCM by 8.8%
- the maximum COP in the case of the solar collector with PCM is 22.7, while the maximum COP of the collector without PCM is 21.77
- due to the presence of phase change materials, during the heating / charging period, the collector with PCM has a slightly lower average COP than the solar collector without PCM: 19.7, compared to 20.3. Obviously, during the cooling / discharge period, the collector with PCM has an average COP up to 4 times higher than the solar collector without PCM: 1.7, compared to 0.4
- when the COP value of the solar collector falls below 1, heating with an electric battery becomes more economically advantageous. Therefore, from 457th minute the solar collector without PCM should be turned off, while the solar collector with PCM should be turned off from 937th minute, when the COP reaches values bellow 1, although it can still provide thermal energy
- the COP of the PCM collector is lower in the first part of the study, because the phase change materials stores energy, while after the solar radiation is stopped, the COP is considerably higher in favour of the collector with PCM

- the average COP of the solar collector without embedded phase change materials is 6.6, while the average COP of the solar collector with embedded phase change materials is 7.3, respectively 10.6% higher
- the overall efficiency of the solar collector is 10.6% higher in the case of the collector with PCM
- during the heating / charging period the energy is stored faster (melting process is obvious between 60th and 240th minute), while the solidification process occurs more slowly, on the whole cooling / discharge stage, with a period in which the process is more intense (between 400th minute and 660th minute)
- the useful operating time (when the COP has values above 1) of the solar collector without PCM is 434 minutes, while in the case of the collector with PCM it is 937 minutes, resulting in a longer operation period of 110% (479th minutes more).

Taking into account the conclusions of the present study we can conclude that the implementation of phase change materials in solar collectors can increase the overall efficiency of the system, the number of operating hours and even the temperature difference between ambient and exhaust air. Moreover, within the study in transient regime, an improvement of exhaust air temperature variations could be observed, the amplitude of temperature variations being lower in the case of using PCM. This transpired solar collector could be implemented in different situations and with different purposes: air preheating, space heating, air drying, air preheating which then enters a heat recovery unit and can be implemented in different applications: residential sector, industrial halls, storage halls, production halls etc., as could be seen in the applications presented within the bibliographic study. Further in-depth experimental studies are needed for longer periods of time and several other sensors must be installed in order to better analyse temperature variations in the first air cavity. It is also necessary to study solar collectors in transient regime, in real operating conditions and in different climatic conditions for longer periods of time (minimum one year of operation). All these studies will be the subject of post-doctoral studies. Also, in the following studies it is necessary to carry out a complex parametric study in order to optimise the design of the solar collector by analysing:

- different air flows
- different types of PCMs for different applications
- the optimum placement of the PCM obstacle inside the cavity
- different designs of the solar collectors and different designes of the PCM recipients
- the impact of absorbent plate orifices on the solar collector.

<u>Capitolul 3 - Modelarea numerică a colectoarelor solare cu aer cu materiale cu schimbare de fază integrate</u>

3.1. Objectives of the numerical studies and hardware used

According to the studied literature, for the numerical study of the transpired solar collectors, respectively for the study of the integration of phase change materials in active or passive systems, many researchers used ANSYS Fluent, CFD (Computational Fluid Dynamics) software.

Many researchers have turned their attention to experimental studies on the implementation of phase-change materials in building [15-23]. However, in order to choose the proper PCM and a proper geometry for a specific application in a building the numerical approach is mandatory [24] due to the complexity of the phenomena occurring in the melting / solidification process. The problem that arises is due to the non-linear character of the phenomena and the fact that the two phases, solid and liquid, have different thermophysical properties [25].

Therefore, according to the above mentioned arguments, I have decided to use the ANSYS Fluent CFD Numerical Simulation Software in order to study solar air collectors with integrated phase change materials. CFDs are based on the fundamental equations governing fluid dynamics: the continuity equation, the energy conservation equation and the impulse conservation equation. Because the results of Navier-Stokes equations cannot be solved analytically, the CFD software tries to find an approximate solution by spatial meshing methods that convert partial-derivative equations into algebraic equations (calculations are iterative).

The steps of a CFD numerical simulation that were followed in the present paper are:

- Creating the geometry of the model
- Creating the calculation grid mesh independency study
- Imposing boundary conditions and configuring the numerical case
- Validating the numerical model by comparing the numerical results with the experimental ones
- Calculation of the solution and post processing

According to the bibliographic study, the implementation of phase change materials in transpired air solar collectors has not been studied so far. The purpose of the current numerical study is to create a numerical model that accurately simulates the air flow through the solar collector with PCM and the transfer phenomena that take place inside it. With this purpose, the designing of the numerical model involves two stages:

- *Numerical modelling of air flow through the lobed orifices (absorbent plate)*
- Designing the numerical model of the solar collector with integrated phase change materials.

The following subchapters cover the two steps presented above. The numerical modelling of the air flow through the lobed orifices aims to study all the complex phenomena that take place when the air flows through them and the analysis of the orifice geometry impact on the solar collector. Simulating the solar collector to its real dimensions would involve a very long computing time due to a very large number of mesh cells, a time that would be practically unfeasible for the completion of studies. The temperature profiles and velocity fields thus obtained from the first numerical study will be integrated into the numerical model of the solar collector with PCM (second numerical study).

The ANSYS Fluent 15.0 CFD numerical simulation software and all its components were used in order to perform the numerical study: ANSYS DesignModeler, ANSYS Workbench and ANSYS Mesher. Tecplot 360, Notepad and Microsoft Excel were used for data processing and the C++ programming language was used in order to realize the variation functions of certain parameters used for the study in transient regime (the ANSYS Fluent compiler is MS Visual Studio C++). Also, two computing stations from the Faculty of Building Services Engineering were used.

3.2. Numerical modelling of air flow through the loved holes (absorbent plate) – the first numerical mode designed

In order to be able to perform the numerical modelling of the solar collector with lobed perforations with integrated PCMs in a feasible period of time, we have simplified as much as possible the geometry of the absorber plate that is part of the solar collector, starting from the premise of the thermal transfer phenomena symmetry and velocity fields symmetry. As it could be observed from the literature, the shape of the orifices considerably influences the efficiency of the solar collector [26, 27], it can improve thermal transfer and can cause a higher air temperature in the collector cavity. The unconventional lobed geometry of the absorbent plate orifices determines complex airflows thus improving the heat transfer and according to the literature is the geometry that helps to obtain the greatest rise in temperature between the ambient air (inlet) and the exhaust air (outlet). The orifices layout in the case shown in Figure 14 is also the most efficient solution for large values of the airflow. Taking into account all these arguments, I decided to consider the effect of orifices on the solar collector flow and efficiency. Moreover, this approach will create future premise of studies regarding the orifices influence on the PCMs integration.

Figure 18 shows the layout and geometry of the lobed holes. The orifices are alternately positioned horizontally (+, x, +, x, +... etc.) at a pitch of 20 mm and with an equivalent diameter of 5mm.

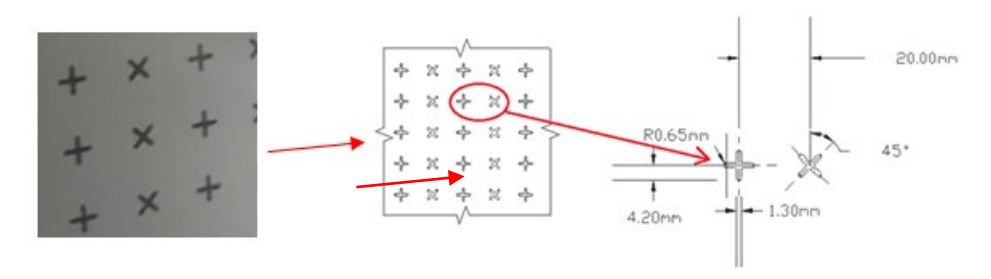


Figure 18. Lobed orifices layout and geometry with equivalent diameter of 5mm (De=5mm)

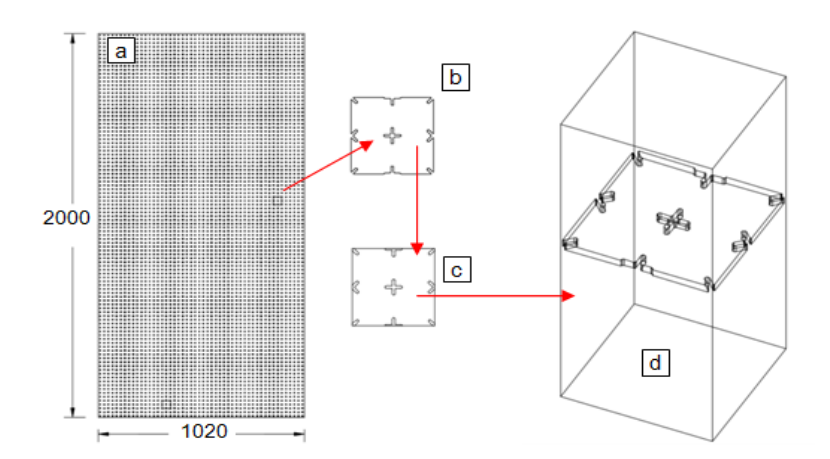


Figure 19. Designing the 3D model in AutoCAD: a – absorbent metal plate with lobed orifices, b – extraction of a 4x4cm part, c – embedment in the computing domain, d –3D computing domain (4x4cm plate surrounded by a parallelepiped)

As can be observed in Figure 19a, the absorbent plate with a surface area of approximately $2m_2$ and a thickness of 2mm has a large number of lobed orifices on its entire area (5000 holes). Modelling the entire absorbent plate with lobed holes would require a complex mesh and a large number of mesh cells in the computing domain in order to accurately capture the phenomena that occur near the orifices. This would lead to a very long time necessary in order to carry out the numerical studies. Taking into account airflow symmetry and transfer phenomena symmetry we selected a 4x4cm metal plate containing 4 equivalent orifices for the present study (Figure 19b).

The 4x4cm extracted metal plate was then enclosed in a 9.2x4x4cm parallelepiped that will represent the airflow in the computing domain, with respect to the flow direction (Figure 19c and 19d). The plate is positioned at 4cm distance from the computing domain limit (inlet - upstream) and at 5cm distance from the outlet (downstream) which represents ten equivalent equivalents (10De=5cm). From the experimental studies carried out at the Faculty of Building Services Engineering we noticed that after 10De, in the case of lobed orifices the airflow and velocity profiles are stabilizing. The velocity fields thus obtained at a distance of 5cm from the metal plate will then be used (introduced as boundary limits on the inlet) into the simplified large-scale numerical model of the solar collector. Figure 20 highlights the geometry and computing domain for the first numerical study conducted.

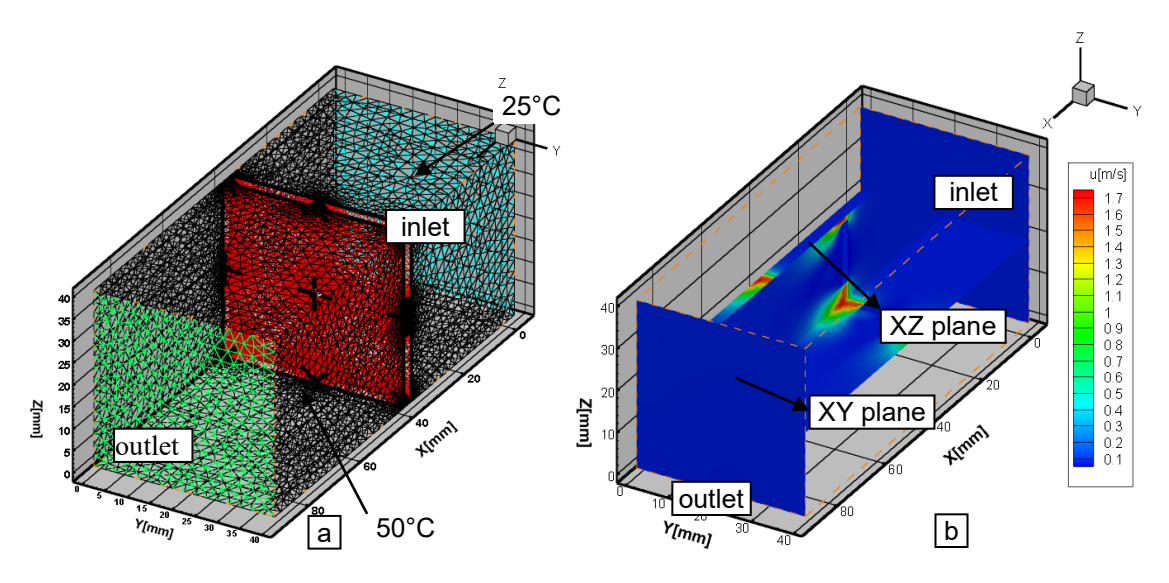


Figure 20. Geometry and computing domain

According to the mesh independency study conducted, we chose the geometry of 5.3 million tetraedral cells because it is an independent solution to the computing grid and this will be used in the numerical model analysed thus being a solution that doesing influence the results of the numerical simulations (figure 21).

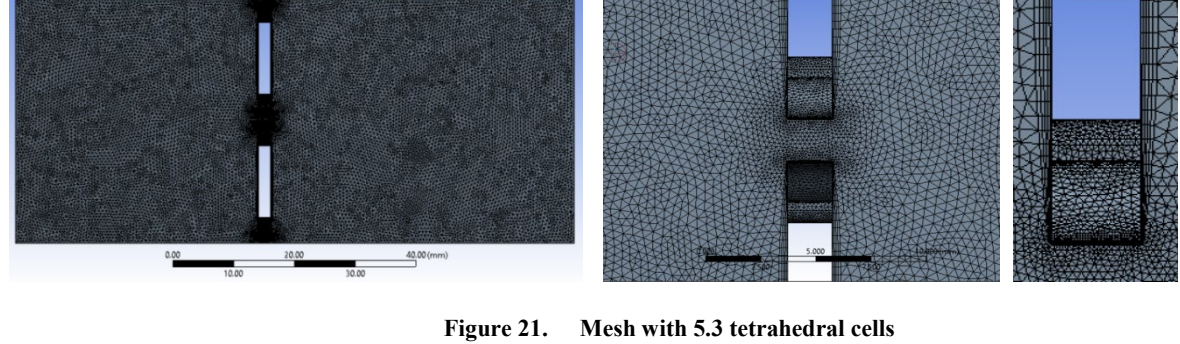


Figure 22. Velocity fields (a) and temperature fields (b) obtained in XY longitudinal plane

We also chose the energy transfer model that takes into account the energy conservation equation and the k- ϵ RNG turbulence model (with EWF) which according to the literature is suitable for the type of flow studied. Having the temperature values at different points following the experimental study, we did not use the radiation heat transfer model in order to obtain a simplified model and to reduce the time needed to obtain useful results. This model will be developed in the future and will be the basis for further post-doctoral studies.

For the air flow within the computing domain I chose from the ANSYS Fluent software database the corresponding properties, also for the metal absorbent plate I chose as material aluminum. The boundary conditions imposed are those presented in Table 2, but they can be modified in order to obtain various results and to perform parametric studies (post-processing of the model itself).

Table 2. Boundary conditions used in the mesh independency study

Boundary limit	Value	Unit
Average velocity at the computing domain limit (velocity inlet)	0.05555	m/s
Inlet temperature (inlet)	25	°C
Metal plate temperature (metal)	50	°C

The interpolation scheme used is "second order upwind" for the analysis of convective terms and the pressure-speed coupling scheme is determined by the "SIMPLE" algorithm. According to the studied literature, the convergence of the solution is achieved when the non-dimensional residuals of the flow equations are less than 10^{-3} ; as a result, in order to obtain the relevant results we have imposed a value less than 10^{-5} .

The numerical model was experimental validated by using two methods: by comparing the velocity fields in longitudinal plane and by comparing the obtained temperatures. The output data from this model will be input data for the next model of the real-size large-scale solar collector.

Obtaining velocity and temperature fields as a result of orifices geometry at 10De will create further opportunity to continue doctoral studying. With these results, we can translate into the numerical model of the solar collector the real impact of the lobed geometry. Also, in the future, we will be able to analyse the impact of the orifices on phase change materials implemented in solar collectors. In the next chapter it will be presented the numerical model of the solar collector with lobed orifices and integrated PCMs. The results obtained in this chapter by using the studied numerical model will be integrated into the real-size model and will constitute input data in the computing domain (inlet of the new model).

3.3. Creating the numerical model of the solar collector with lobed orifices and integrated phase change materials – simplified model

3.3.1. Creating the simplified numerical model of the real-size solar collector

After realizing the numerical model analysing the airflow through the lobed orifices (absorbent plate) I continued with the actual modelling of the solar collector with integrated phase change materials. The velocity and temperature fields resulting from the model studied in the previous chapter (outlet at 10De) will constitute input data for the new numerical model (inlet), as shown below. In order to achieve the numerical simulations within a feasible time period, we decided to simplify the real geometry, starting from the premise of the symmetry of the phenomena which are composing the entire collector. Figure 23 shows the absorbent plate through which ambient air is aspired into the solar collector cavity. From this we extracted a row of orifices (Figure 23a), resulting in a "transversal slice" through the solar collector (Figure 23b). Aspiration (collectors' inlet) is composed of 50 plates with 4x4cm lobes studied in the previous chapter and has the dimensions of 4x200cm. The air circulated through the collector with the properties set at 10De is aspired into the new model, enters the cavity between the metal plate and the phase change materials obstacle, continues the downstream trajectory due to the PCM chicane and after reaching the bottom of the collector will follow an ascending trajectory that ends with the outlet of the air from the solar collector. The dimensions of the "slice" respect the real geometry of the solar collector with integrated PCMs.

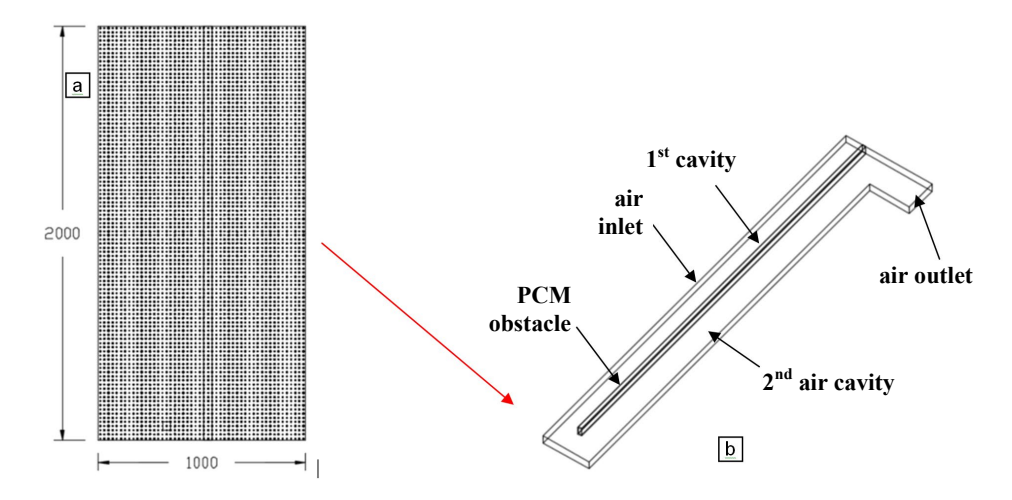


Figure 23. Designing the geometry in AutoCAD: a – absorbent plate with lobed orifices, b – extraction of a "slice" from the solar collector and its components

Modelling of the entire solar collector would involve a complex spatial meshing or a very large number of cells in the computational grid in order to accurately capture the phenomena that take place. After realizing the solar collector geometry in the AutoCAD design software, the 3D model was saved in .igs and imported into ANSYS DesignModeler. The inlet of the solar collector was divided into 50 x 4 x 4 cm faces in order to integrate the velocity fields obtained at 10De from the lobed orifice plate studied in the previous chapter (Figure 24).

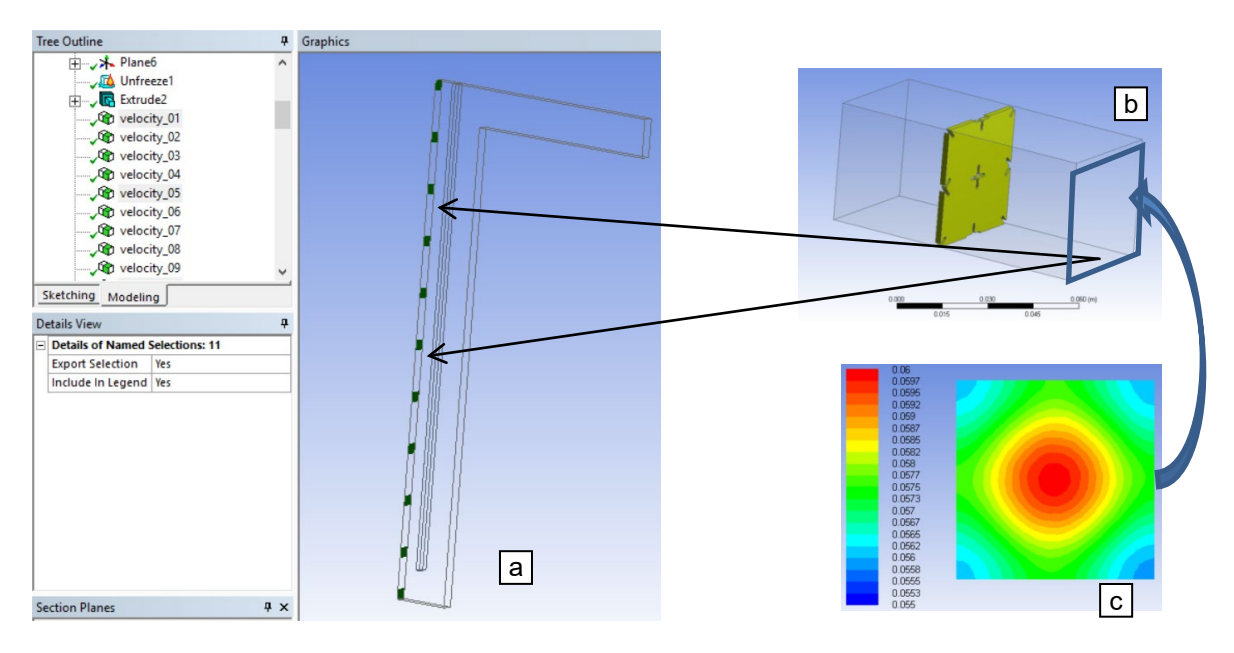


Figure 24. Creating specific air intake areas (inlet) where the velocity and temperature profiles from the previous chapter will be entered: a – 50 zones on the inlet; b – the outlet of the previous study became the inlet of the new study; c – velocity field which will be integrated on the new inlet

3.3.2. Creating the optimum mesh (mesh independency study)

Similar to the steps followed in the previous chapter, after the proper construction of the geometry, the next step of the numerical modelling is choosing the optimum mesh. Moreover, in order to determine the number of computational elements (cells) needed to solve the problem, it is necessary to make a solution independency study with respect to the quality of the meshing.

In order to conduct the mesh independency study I chose also 6 meshing levels, respectively: 0.2, 0.66, 1.3, 2.8, 5 and 6 million cells. In order not to carry out the mesh study in transient regime, which would substantially extend

the time needed for the present study, we decided to remove the PCM layer from the model and carry out the study in steady state regime. This will not affect the final result because we aim to study the airflow through the solar collector with PCM and the resulting temperatures (and not the phenomena that occur in the PCM cavity). By extracting the PCM cavity form the entire geometry, results the following meshing levels: 0.18, 0.61, 0.7, 1, 2.5 and 3.5 million. The optimal meshing level is established by conducting individual numerical simulations, using boundary conditions and identical calculation models.

The six meshing levels were then imported in ANSYS Fluent and for each of them the same boundary conditions were imposed, which are shown in Table 3. The inlet air velocity corresponds to the velocity profiles obtained from the previous study and has values ranging from 0.055 to 0.06 m/s for each of the 50 faces, resulting in a total velocity in the "slice" of about 2.75 m/s. The temperature of the air at the inlet (at 10De) is 26 °C and the temperature of the wall which separates the PCM layer to the cavity is 40 °C. These assumptions represent the cooling stage, respectively the heat transfer from the PCMs to the airflow in periods when the solar radiation isn't available.

Boundary conditionValueUnitVelocity magnitude (inlet)Velocity field obtained from the previous study with values
between 0.055-0.06 m/s for all 50 faces on the inletInlet temperature (inlet)26°CPCM temperature (wall between the PCM and the cavity)40°C

Table 3. Boundary conditions used in the mesh independency study

The velocity field obtained at 10De in the previous chapter was imported in the Tecplot data processing software. On this I created a matrix of points that were subsequently exported to Notepad and processed in X, Y, and Z coordinates so that they could fit into the new model's coordinates. The newly created profiles were subsequently imported and retrieved under the boundary conditions in the inlet area.

In addition to the energy conservation model, I chose the k- Ω SST turbulence model (with corrections for a small Reynolds numbers as the case studied and curvature corrections etc.). This is one of the most feasible turbulence models and is suitable, according to the literature, for small Reynolds numbers [28] and for airflows within rectangular air cavities [29]. Although experienced CFD researchers recommend the analysis of multiple combinations of meshing levels and turbulence models, the reduced time available for the present study didn't allowed us to compare several models of turbulence in this case [30]. With respect to the above mentioned data, we have performed numerical simulations for the 6 computational grids and obtained interesting results.

Following several numerical simulations conducted for the 6 meshing levels chosen, it can be observed that for 0.2 and 0.66 million cells the temperature distribution is relatively similar and uniform and starting with 1.3 million cells it begins to change. However, starting with the 2.8 million cells, the temperature distribution begins to normalize again, while at 5 million and 6 million cells the results are virtually similar. It can be seen that at the bottom of the solar collector, the air flow temperature is higher due to the appearance of vortices and air circulation at a relatively low velocity, seen also at the top of the secondary cavity. In the zones where the temperatures are lower we can observe also high values of air velocities.

Following several numerical simulations conducted for the 6 meshing levels chosen, it can be noticed that for 0.2 and 0.66 million cells the velocity distribution is relatively similar and uniform, while starting with 1.3 million cells it changes similarly to the temperature field. However, starting with the 2.8 million cells, the velocity distribution begins to stabilise, while the results of 5 million and 6 million cells are virtually similar. It can be also observed that at the bottom of the solar collector in the second cavity, the air velocity near the wall increases because of the PCM obstacle presence which causes the apparition of vortices in the vicinity of the chicane and determines the temperature to increase.

In order to conclude, after conducting the mesh independency study, taking into account the above-mentioned aspects, I decided to continue by using the 5 million element mesh because it determines a mesh independent solution (figure 25).

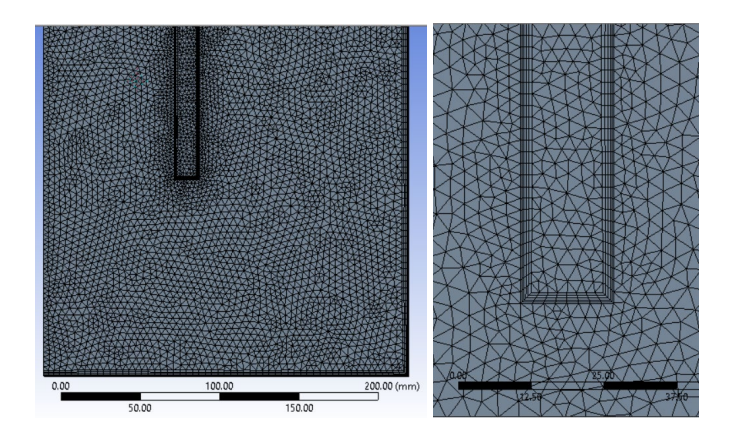


Figure 25. The mesh which will be used – the final case with PCM (5 million elements)

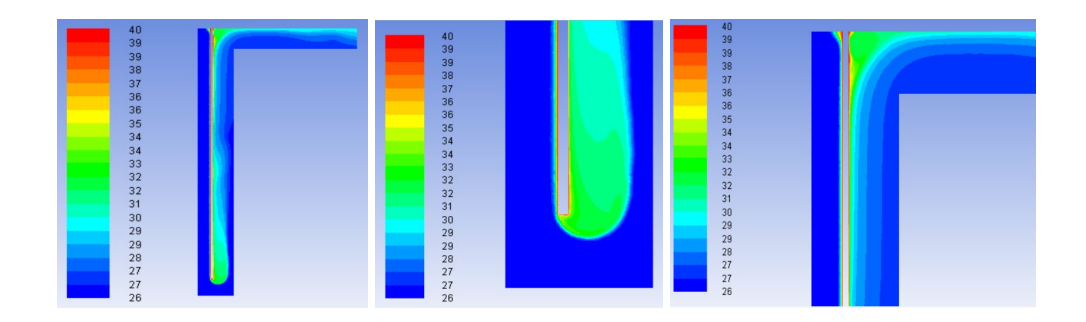


Figure 26. Temperature fields in longitudinal plane (symmetry) – for the mesh with 5 million elements

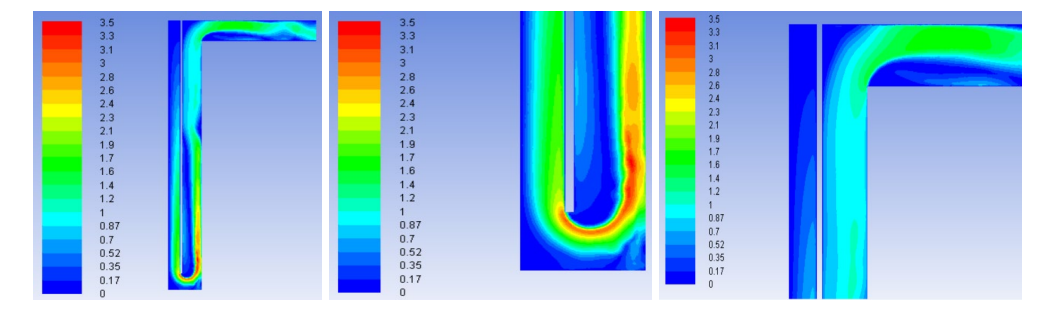


Figure 27. Velocity fields in longitudinal plane (symmetry) – for the mesh with 5 million elements

3.3.3. Experimental validation of the numerical model – comparison of the temperature variation

After the mesh independency study presented in the previous chapter, the experimental validation of the numerical model of the solar collector with lobed holes and embedded phase change materials will be conducted. Validation will be realised in two stages. In the first stage we will obtain the temperature variation on 10De in transient regime using the model analysed in Chapter 4 and we will compare it with the measurements made. The temperature variation at 10De will then be imposed on the large scale model (the "slice" through the collector) as boundary conditions.

After the validation in transient regime of the numerical model analysing the airflow through the metal plate with lobed orifices, the experimental validation of the solar collector model with integrated phase change materials follows. In this regard, at the geometry and mesh created for the air cavity I added the geometry and mesh related to the phase changing materials (Figure 28). The result is a mesh made of 5 million cells (2.5 million for the air cavity and 2.5 million the PCM).

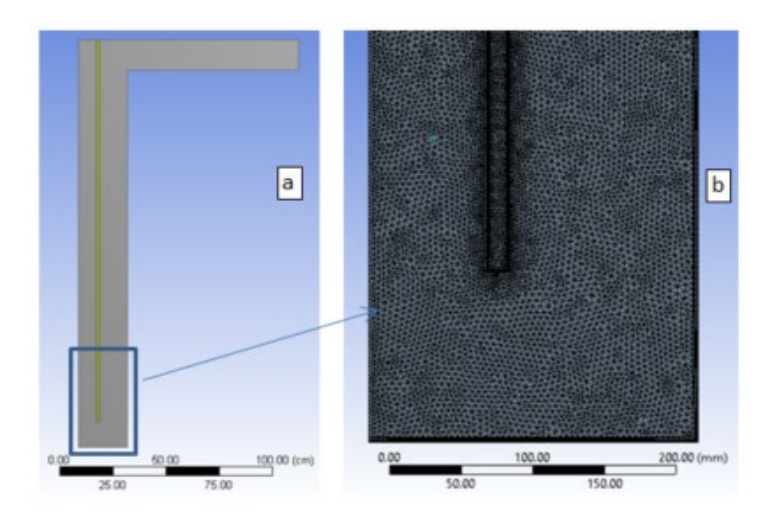


Figure 28. a - the geometry of solar collector with PCM and b - mesh with PCM (5 mil. cells)

After importing the mesh into the Fluent solver I began to set the numerical model case. Therefore, I activated the model using the energy conservation equation and the k- Ω SST turbulence model according to the previous chapter. The next step was to define the materials used in the numerical study: air and phase change materials. The air properties were taken from the ANSYS Fluent database. For the PCMs we used paraffin RT35 properties presented in Table 1 and used within the experimental study. In order to simplify the numerical model, we first considered that the PCMs are solid and have a specific heat capacity variable depending on the temperature. The stored/released energy variation by the PCM at every 1°C variation is presented in figure 2 and it was introduced in ANSYS Fluent as a material variable property. In this manner, the numerical model takes into account the thermal effect of the PCMs, neglecting the phenomenon which occurs in the rectangular cavity, including the effect of natural convection and solidification/melting processes. The storage capacity is presented as a sum of sensible heat and latent heat.

In order to determine the air temperature of the air on the solar collector outlet (T outlet) it is necessary to know the air temperature variation in the 1st cavity at 10De and the initial temperature of the phase change materials. To achieve the experimental validation of the numerical model over a feasible time period, we used the same 120-minute study interval and the experimental results being highlighted in Figure 29. In order to impose as boundary condition at the inlet the temperature variation at 10De we used the experimental results instead of the numerical ones presented above, which are practically similar. In order to run the numerical simulation, it is necessary to measure also the temperature of the PCMs, therefore another temperature sensor was added to the experimental setup in order to measure the temperature on the PCM recipient. To create the program that describes the temperature variation at 10De in the C++ protocol it is necessary to split the results in three stages, similar with the

previous case. The first stage of temperature variation – heating is characterized by a linear variation, the second stage of the 10De zone temperature variation coincides with the sudden stop of the lamps that simulate the solar radiation which determines a rapid temperature drop and it is characterized by a 4th degree polynomial equation. Finally, the third stage of temperature variation – cooling is also characterized by a 2nd degree polynomial equation and describes a slow discharge. After obtaining the three equations needed, we have implemented the C ++ program which will determine the introduction of variable boundary conditions in the numerical model realized in Fluent.

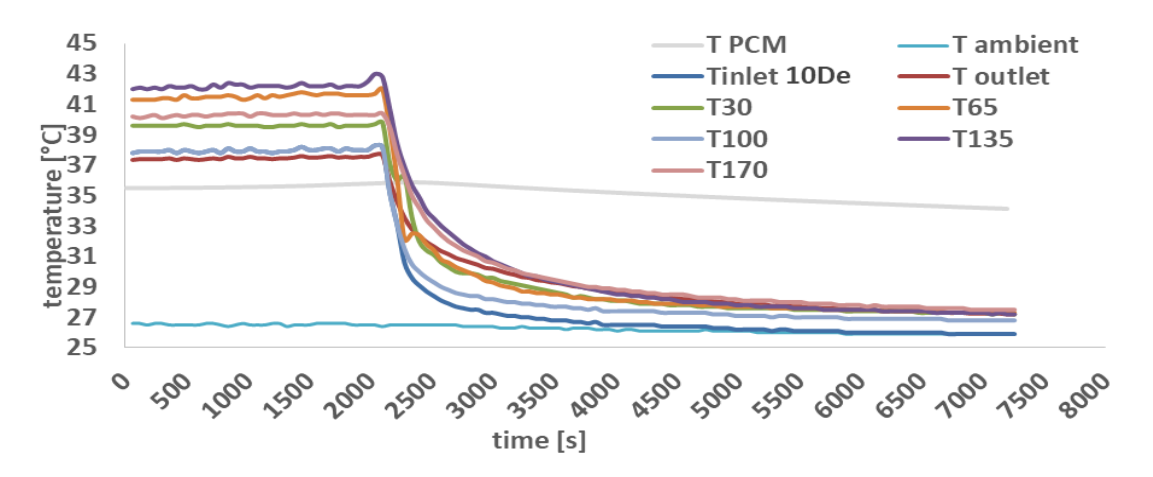


Figure 29. Variația de temperatură pentru două ore

The boundary conditions used within the numerical study conducted are shown in Table 4. Temperature variation at 10De is determined by the UDF presented above and the velocity fields were imported for the 50 faces as a result of the study presented in Chapter 4. Moreover, temperatures were also monitored in different points of the numerical model solar collector as well as the average surface temperatures. The Fluent Solver gives the possibility of setting an initial temperature for a particular material. The initial temperature in the present case for PCM is 35.5 ° C ("patch" function in the initialization), with respect to the experimental results.

Table 4. Boundary conditions used in case of experimental validation of the solar collector with integrated PCMs

Boundary condition	Value	Unit
Velocity magnitude (v inlet 10De)	Velocity field obtained from the previous study with values between 0.055-0.06 m/s for all 50 faces on the inlet	
Inlet temperature (T inlet 10De)	Variation imposed by the UDF created (user defined function)	
PCM temperature (valoare inițială impusa)	35.5	°C

In order to start from a stable solution I ran the simulation in the permanent regime and after stabilizing the solution I set the case for the numerical simulation in the transient regime imposing the following case conditions: 10s time step, 720 steps (7200 seconds) and 20 iterations on each time step. In addition to these settings, the case was also run for 1s, 5s, 10s, and 20s, respectively for 10 iterations, 15 interactions, 20 iterations, and 30 iterations. The conclusions were as follows: over 10s and less than 20 iterations, the phenomenon is not accurately rendered especially for the second stage of temperature variation (II).

In order to achieve the experimental validation of the numerical model of the solar collector with embodied PCMs I chose to compare the air temperature in the 2^{nd} air cavity, in the middle of it at 100cm from the bottom part of the collector (T100). In figure 30 it is emphasised the T100 temperature variation both for the numerical study and experimental study.

Moreover, in order to validate the numeric model I also chose to compare the values obtained in the numerical study and in the experimental study for the air temperature variation at the collectors' outlet (Toutlet). In figure 31 we can observe the overlapped results. The temperature variation at 10De respects the variation imposed by the UDF created. Moreover, the allure of the exhaust air temperature variation curve (Toutlet) obtained in the case of

numerical simulation is similar with the one obtained in an experimental manner with small differences that can be determined by the fact that the numerical model is a simplified one and doesn't comprises all the solar collector components which can contribute to the thermal inertia of the systems (e.g.: OSB, thermal insulation etc.). By comparing the values obtained experimentally with the ones achieved in a numerical manner we can conclude that the numerical model created reproduces the real heat transfer phenomena within acceptable limits.

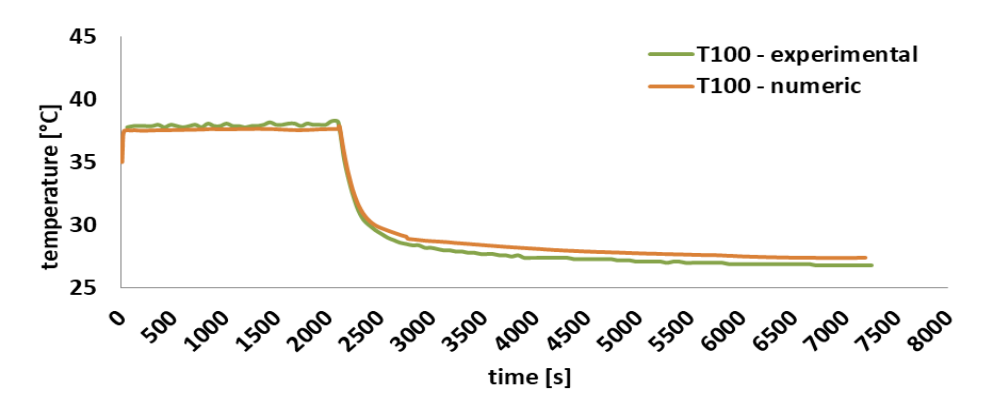


Figure 30. Results of the numerical study vs. experimental study at T100

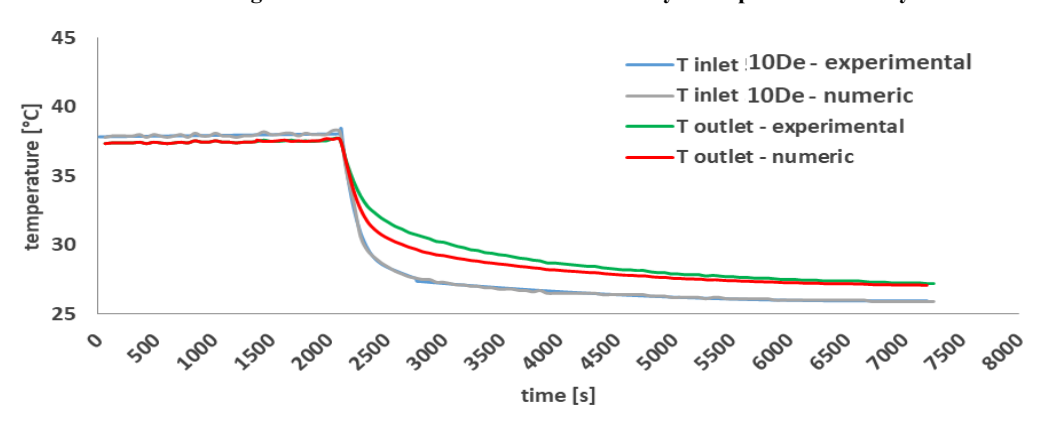


Figure 31. Results of the numerical study vs. experimental study: Toutlet and Tinlet

3.3.4. Final parameters of the numerical study vs. experimental study: Toutlet and Tinlet

By considering the analyses elaborated in this chapter, we can conclude the final parameters of the numerical model that studies the solar collector with integrated phase changing materials. The geometry is based on a simplified concept which represents a slice through the solar collector, the inlet in the computing domain consisting of 50 faces whose boundary limits (especially velocity fields) where obtained from the model that studies the airflow through the absorbent metal plate with lobed orifices. According to the mesh independency study the geometry with 5 million tetrahedral cells has resulted to be the one that will not influence the results of the numerical simulations while being a stable solution. The mesh presents 2.5 million cells in the solar collectors' air cavity and 2.5 million cells in the PCMs enclosure.

The energy conservation model and $k-\Omega$ SST turbulence model (with corrections for a small Reynolds numbers as the case studied and curvature corrections etc.) have been chosen for the numerical case. According to the literature this kind of turbulence model is suitable for the time of airflow studied. Having the temperature values at different points from the experimental study, we did not use the heat transfer model for radiation in order to obtain a simplified model and to facilitate as much as possible the calculations. This model will be developed in the further studies and will underpin the continuation of post-doctoral studies. For the air circulated in the computing domain I chose from the ANSYS Fluent database the corresponding properties, moreover regarding the PCMs I introduce the paraffin RT35 characteristics and I considered that the material is in solid state having the specific heat variable with temperature. Although the melting and solidification processes cannot be studied in this case, the thermal

impact of PCMs is reproduced with accuracy. For the variable boundary conditions I used the velocity profiles obtained in the previous model and in order to study the collector in transient regime I have imposed user defined functions (UDFs) create in C++ programming language. Furthermore, for initialization I have imposed an initial temperature for the PCM.

The interpolation scheme used is "second order upwind" for the analysis of convective terms and the pressure-speed coupling scheme is determined by the "SIMPLE" algorithm. According to the studied literature, the convergence of the solution is achieved when the non-dimensional residuals of the flow equations are less than 10^{-3} ; as a result, in order to obtain the relevant results we have imposed a value less than 10^{-5} .

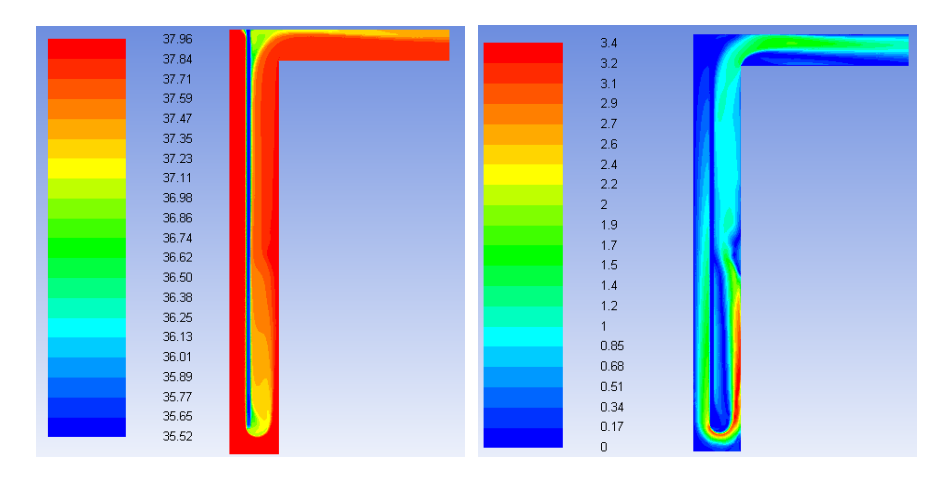


Figure 32. The results of the numerical study in transient regime after 1200s: a – temperature field, b – velocity field

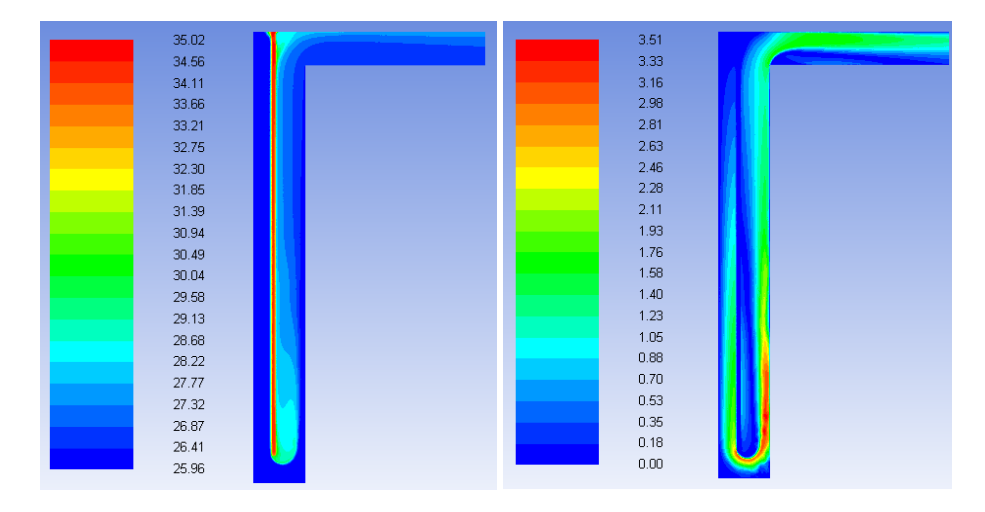


Figure 33. The results of the numerical study in transient regime after 7200s: a – temperature field, b – velocity field

Figure 32 and Figure 33 highlights temperature and velocity fields for the solar collector after different time periods from the numerical study conducted.

3.4. Conclusions and perspective of the numerical studies conducted

According to the bibliographic study, the implementation of phase change materials within solar collectors has not been previously studied with both an experimental and numerical point approach, as there is no numerical model to simulate the phenomena that take place inside the collector. The numerical study is quite difficult to perform due to the large number of orifices of the absorbent plate and due to the complex phenomena that take place inside the solar collector. Therefore, the present study proposes the analysis of a simplified numerical model, but which was experimentally validated. The numerical study is therefore divided into two stages:

- numerical modelling of the air flow through the lobed orifices, model that analyze the flow through a part of the absorber plate of the collector (4 holes)
- numerical modelling of the real-scale collector (study of the airflow through a "slice" of the real-scale solar collector).

The output data from the first numerical study represent input data for the second numerical model created. The numerical modelling of the air flow through the lobed orifices has the purpose to correctly understand and recreate the phenomena that take place when the air flows through them and to analyse of the impact of the orifice geometry on the collector. Simulating the solar collector to its real dimensions would involve a very long computing time due to a very large number of cells mesh, a time that would be practically unfeasible for the completion of studies. The temperature and velocity fields thus obtained from the first study were therefore integrated into the numerical model of the real-scale solar collector with integrated PCM. After creating the numerical model that analyses the air flow through the lobed orifices (absorbent plate) we continued with the modelling of the actual solar collector with integrated phase change materials. The velocity and temperature fields resulting from the first model (10De outlet) will be input data for the new numerical model (inlet). The modelling of the entire solar collector would involve a complex spatial discretization, respectively a very large number of cells within the computing grid in order to accurately recreate the phenomena that take place.

The first model studied that analyses the air flow through the lobed orifices presents, according to the study of the independence of the solution from the discretization quality, a mesh with 5.3 million tetrahedral elements that do not influence the results of numerical simulations, being a stable solution. For this model we chose the energy transfer model that takes into account the energy conservation equation and the k- ϵ RNG turbulence model (with EWF) which according to the literature is suitable for the type of flow studied. Having the temperature values at different points following the experimental study, we did not use the radiation heat transfer model in order to obtain a simplified model. This model will be developed within further studies and will be used in postdoctoral studies. For the air circulated within the computing domain we chose from the database of the ANSYS Fluent software the corresponding properties, also for the metal absorbent plate we chose as material aluminium and boundary conditions according to the experimental data. This model was experimentally validated in two ways: by comparing the velocity fields in the longitudinal plane and by comparing the temperatures obtained within in the solar collector cavity. Having these results, we can transpose to the numerical model of the solar collector the real impact of the lobed orifices.

The geometry of the second numerical model of the large collector is based on a simplified model that represents a "slice" through the solar collector, the input into the computing domain being made up of 50 faces whose boundary conditions, in particular velocity fields, were taken from the model that analyses the flow through the metal plate with lobed holes (the first model made). According to the mesh dependency study, a geometry with 5 million tetrahedral elements resulted that does not influence the results of the numerical simulations, being a stable solution. The mesh has 2.5 million cells in the area of the air cavity and 2.5 million cells in the area that delimits the phase change materials. We also chose the energy transfer model that takes into account the energy conservation equation and the $k-\Omega$ SST turbulence model (with corrections in case of a small Reynolds number and corrections in case of flows where there are obstacles, bends etc.) which according to the literature it is suitable for the type of flow studied. Having the temperature values at different points following the experimental study, we did not use the radiation heat transfer model in order to obtain a simplified model that will facilitate further simulations. This model will be developed within further studies and will be the basis for the continuation of post-doctoral studies and parametric studies that will optimize the studied solar collector. For the air circulated withinin the computing domain we chose from the database of the ANSYS Fluent software the corresponding properties, also for the phase change materials we imposed the characteristics of the paraffin RT35 and we considered that the material is in solid state with variable specific heat depending on temperature. Even if the melting and solidification processes cannot be studied at the moment, the thermal impact of the phase change materials is well reproduced. The second model was experimentally validated by comparing the variation of temperatures, in a transient regime. Numerical studies have shown the vortices created in the second air cavity that cause an unusual thermal stratification created by the introduction of the obstacle with embedded PCMs.

The model created will further studied and developed in post-doctoral studies, the current one thus being a simplified one. It will be the basis for complex parametric studies useful for the optimization of the solar collector that will analyse different types of PCMs, different geometries of the orifices, different positions of the obstacle with PCM, different airflows etc.

<u>Chapter 4 – Conclusions and perspectives of the current paper – personal contributions</u>

This paper exhaustively analysis the implementation of phase change materials within transpired air solar collectors, both from an experimental and a numerical perspective while performing a comprehensive analysis of the state of art in the field studied.

The first chapter of the paper is represented by a complex bibliographic study that analyses, one by one, the implementation of phase change materials in buildings and buildings systems and the integration of the two principles, respectively the incorporation of phase change materials within solar air collectors and the potential of the new propped system on reducing energy consumption and operating costs of a building. Recently, there has been an upward trend and a particular focus of researchers on the implementation of phase change materials in buildings and building systems, more and more scientists being interested in their impact and the confidence of the research community is increasing by understanding better and better their potential. However, current costs are still high due to a relatively small number of existing producers on the market, being still a niche market. According to the studied literature, phase change materials have the advantage of storing a big amount of energy at a small temperature variation and at values of operating temperatures very close to the level of thermal comfort or the temperatures required in building systems. These materials have over time been integrated into construction elements, plasterboards, solar systems or buffer tanks, ventilated facades or in active ventilation systems. Recent studies show that phase change materials can easily be part of passive or active strategies used in order to reduce energy consumption and improve thermal comfort in buildings, with remarkable results, as they can be part of the envelope elements of the building or its heating, cooling and ventilation systems. Transpired air solar collectors are a cost-effective alternative to more intensively studied opaque or glazed solar collectors (e.g. the "Trombe" wall), while air solar collectors can generally be a more viable solution in comparison to well-known water thermal collectors thus having no risk of frost and having low operating costs. However, due to the difficulties determined by the lack of thermal storage solutions, solar air collectors are still rarely implemented in real applications, being especially successful in North America and North Africa. Air solar collectors could be implemented in any type of application, but so far they have been used in the industrial field: production halls, storage halls, vegetable and fruit storage halls, in order to maintain a guard temperature or to dry vegetables. According to the bibliographic study performed, phase change materials can be implemented in solar air collectors, increasing their overall efficiency and number of operating hours, thus contributing to space heating or preheating of fresh air introduced into rooms. Moreover, the increase in thermal inertia of the collectors can lead to the improvement of temperature variations in the case of the air exhausted from the collector to the indoor environment or to a heat recovery unit. Therefore, the implementation of phase change materials in solar air collectors can lead to the accumulation of energy during the day, when solar radiation is available and its use during cloudy periods or at night, when the solar radiation is no longer available.

According to extensive bibliographic studies identified [11, 12, 31-34] systems consisting of transpired opaque air solar collectors and integrated phase change materials haven't been studied until now. Following the bibliographic study conducted, no studies were identified in the literature on the implementation of phase change materials for energy storage in perforated solar collections used as an exterior wall in the building envelope. Also, there has not been identified in the literature a numerical model used to analyse solar collectors with lobed geometries, nor transpired solar collectors with integrated phase change materials. Therefore, a first personal contribution consists in the extensive bibliographic synthesis made in the chapter that analyses the current state of art in the field studied, given all the aspects listed above and the lack studies identified in the literature focused on the integration of PCMs

in air solar collectors. This study opens new perspectives and research opportunities in the field that will be the subject of further doctoral studies.

The second chapter of the paper refers to the experimental analysis of the integration of phase change materials in real-scale air solar collectors that can be integrated into the building envelope or building systems. In order to reach the final prototype studied, it was necessary to conduct many preliminary studies that led to the optimization of the final model. The first experimental study analysed the melting and solidification processes of organic phase change materials (paraffin RT35) macroencapsulated in rectangular aluminium containers. Due to the fact that no containers could be identified on the market that could be integrated in the designed solar collector, we integrated the studied material in aluminium bars, a new encapsulation method that leads to space optimization and the possibility to use a large amount of PCMs. The first experimental study analysed the processes of melting and solidification of phase change materials. This study aimed to validate the chosen constructive solution, to understand the processes that take place inside the PCM containers and to identify their optimal position in the solar collector. The first experimental study concluded that the melting period (heat storage period) is shorter in the case of vertically positioned containers, the thermal stratification inside being obvious. The aluminium used distributes heat evenly due to the increased thermal conductivity and the solidification period of the material is slower than the melting period. The second experimental study focused on testing the newly built PCM containers in small solar collectors already validated in previous studies conducted at the Faculty of Building Services Engineering. The aim of this study was to identify the optimal position of the containers inside the large solar collectors and to observe their impact on the temperature of the air discharged from the collector. The findings showed that phase change materials must be placed in the middle of the cavity to increase the heat exchange surface, the study must be performed over a longer period of time in order to restore the phase change cycle and the implementation of inertial materials has the potential to increase the overall efficiency of the system and the number of operating hours, which is why we moved on to the next study on the large collector. The third experimental study within in the second chapter of this paper deals with the experimental analysis of the large-scale collector with lobed perforations and embedded phase change materials, the first case in which the PCM bars are placed in the middle of the air cavity thus formin a coil (storage battery), with spaces between the containers, as well as with spaces between the supporting metal frame and the walls of the collector. This study highlighted the geometry of the large solar collector that can be used in real applications and concluded that due to the location of the fan at the top of the collector there is a vertical pressure difference that forces air flow especially towards the upper part of the collector, fact influenced also by the pressure drops determined by the positioning of the rectangular containers. Both the thermal stratification and the pressures study confirmed these hypotheses.

Therefore, following the conclusions of the third experimental study, the prototype of the solar collector was optimised and we continued with the fourth experimental study that refers to the implementation of phase change materials in solar collectors with large lobed perforations, in which the layer of PCM forms an obstacle in the middle of the air cavity that guides the flow of air through the cavity. This prototype is the final one adopted and the one that proved to have the best performances. The collector was exhaustive studied in permanent regime in order to observe the impact of the PCMs, but also several preliminary studies were performed in transient regime. Following the experimental study it could be concluded that the rise in temperature in the case of the collector without PCM is maximum 10.2 °C (9.7% more than the case of the collector without the middle obstacle) and the maximum temperature of the air exhausted from the solar collector without PCM is 34.7 °C. The heat transfer is mainly realized in the first air cavity and after the lamps have been switched off, the temperature values are quickly equalizing in the case without PCM. Moreover, the rise in temperature in the case of the collector without PCM reaches a maximum value of 11.1 °C (7.8% more than in the case of the collector without obstacle), while the maximum temperature of the exhaust air from the solar collector without PCM is 37.6 °C. The temperature at the outlet of the collector is lower in the case of using PCM especially in the first part of the studies, when the PCM stores energy and after stopping the solar radiation the energy is slowly yielded to the air flow (in the case with PCM). It can be observed, however, that the thermal stratification is unusual, which may be due to vortices that may occur because of the obstacle placed in the middle of the air cavity (fact confirmed within numerical studies). The maximum rise in temperature, the main parameter analysed in the case of air solar collectors, is higher in case of using PCM by 8.8%.

The melting phenomenon is obvious for 180 minutes, during which the rise in temperature in the case of the collector with PCM is lower than in the case without PCM. Although the second case studied, with the PCM layer that forms an obstacle, shows better results, the heat transfer is slower and the energy discharge occurs slower than in the previous case. During the heating / charging period the energy is stored faster (melting is obvious between 60th minute and 240th minute), while the solidification process occurs more slowly, throughout the cooling / discharge stage, with a certain period of time in which the process is more intense (between 400th minute and 660th minute). The maximum heating capacity of the solar collector without PCM is 1.46kW (0.73kW / m²), while the collector with PCM reaches a maximum of 1.52kW (0.76kW / m², by 4.1% more). During the heating / charging period, the average heating capacity of the solar collector with PCM is 1.32kW (0.66kW / m²), slightly lower than the solar collector without PCM which reaches a value of 1.36kW (0.68kW / m²), which it is due to the energy stored within the phase-changing materials. During the cooling / discharge period, the average heating capacity of the solar collector with PCM is 117W (58.5W / m²), almost 4.7 times higher than the solar collector without PCM which reaches a value of 25W (12.5W / m²), fact which is determined by the energy released by the phase change materials to the air flow through the solar collector. When using PCM, the solar collector produces a maximum of 1.445kWh in one hour of operation (6th hour of operation), while the collector without PCM produces a maximum of 1.397kWh (5th hour of operation). The solar collector with PCM produces on average 484Wh per hour of operation, during experimental studies, while the solar collector without PCM produces on average 440Wh. Within the heating stage the solar collector with PCM produces 7.4kWh, less than the solar collector without PCM which produces 7.6kWh. Within the cooling stage the solar collector with PCM produces 2.3kWh, twice as much as the solar collector without PCM which produces 1.2kWh. The total amount of energy produced by the collector without PCM is 8.8kWh (4.4kWh / m²), while the solar collector with PCM produces 9.7kWh (4.85kWh / m²), respectively with 10.2% more energy within the 20 hours of operation, so both solar collectors with and without PCM have the potential to have a quick return of investment comparing to the use of a conventional electric heating coil. The average heat transfer efficiency of the PCM collector is 34.11%, while the average heat transfer efficiency of the PCM-free collector is 35.6%. This may be due to the fact that part of the amount of energy absorbed by the absorbent metal plate is yielded by the radiation phenomenon to the obstacle containing phase change materials. After the melting period, the heat transfer efficiency is slightly equalizing, the solar collector with PCM reaching the maximum value of 37.54%, while the solar collector without PCM reaches the maximum value of 37.89%. The maximum efficiency of the collector with PCM is 94.97%, while the maximum efficiency of the collector without PCM is 91.17%. However, the average efficiency of the solar collector with PCM is lower during the heating / charging period due to the phase-changing materials that store energy: 83.59%, unlike 85.54% in the case without PCM. During the cooling / discharging period, the efficiency of the solar collector cannot be evaluated as the halogen lamps are switched off, thus simulating the period when the solar radiation is not available. The overall efficiency of the collector can be properly assessed only by analysing the coefficient of performance of the solar collector (COP). The maximum COP in the case of the solar collector with PCM is 22.7, while the maximum COP of the collector without PCM is 21.77. Due to the presence of phase change materials, during the heating / charging period, the collector with PCM has a slightly lower average COP than the solar collector without PCM: 19.7, compared to 20.3. Obviously, during the cooling / discharge period, the collector with PCM has an average COP up to 4 times higher than the solar collector without PCM: 1.7, compared to 0.4.

When the COP value of the solar collector falls below 1, heating with an electric coil becomes more economical. Therefore, from 457th minute the solar collector without PCM should be turned off, while the solar collector with PCM should be turned off from 937th minute, when the COP reaches values bellow 1, although it can still provide more heat. Moreover, the COP of the PCM collector is lower in the first part of the study, because the phase change materials store energy, while after stopping solar radiation, the COP is considerably higher in favour of the PCM collector. The average COP of the solar collector without embedded phase change materials is 6.6, while the average COP of the solar collector with embedded phase change materials is 7.3, respectively 10.6% higher. During the heating / charging period, energy is accumulated faster (melting is evident between 60th minute and 240th minute), while the solidification process occurs more slowly, throughout the cooling / discharge stage, with a period in which the process is more intense (between 400t minute and 660th minute). Therefore, the useful operation time period (when the COP value is above 1) of the solar collector without PCM is 434 minutes, while in the case of the collector with PCM it is 937 minutes, resulting in a 110% longer operating period (479 minutes more). Moreover,

in transient regime, during the day, the amplitude of outlet temperature variation in the case of the collector without PCM is 4.2 ° C, while in the case of the collector with PCM the amplitude of the temperature variation at the outlet of the collector is 2.8 ° C, respectively 33% lower.

Therefore, one of the main original contributions of this study refers to the construction and experimental analysis of the real-scale prototype of the large collector with lobed orifices and with integrated phase change materials, which can be integrated into the facade of a building, a system that has not been studied so far. Moreover, a large solar collector with lobed orifices has not been identified in the literature. The geometry of the rectangular aluminium containers and the combination with paraffin R35 is simple, but at the same time it has not been identified in the studied literature. These simple containers have the advantage of, optimizing the space occupied inside the air solar collector.

All these experimental studies are the basis for future post-doctoral studies that will focus on the study of melting / solidification of phase change materials installed within transparent containers in order to better understand the processes that take place inside. Also, different types of phase change materials integrated in the studied rectangular cavities will be studied experimentally. These newly proposed PCM bars will be able to be implemented not only in solar collectors, but also in the envelope elements of a building or in active systems. Moreover, in-depth parametric studies will be further performed on the large-scale solar collector that will analyse different air flows through the collector, different types of inertial materials, different amounts of inertial materials, their different positions within the air cavity and even different geometries of the orifices or solar collectors. Also, for a relevant ROI calculation and for an analysis confirming the data obtained on in permanent regime, it is necessary to study the solar collectors in a transient regime, in real climatic conditions, for longer periods of time (for example, over a period of one year). However, in the transient regime it is necessary to choose a lower phase change temperature in order to benefit from the phase change cycle even at lower outside air temperatures. Also, better results will be obtained at lower flow rates of the air circulated through the collector.

If from the experimental point of view, the implementation of phase change materials in transpired air solar collectors has not been studied so far, obviously, no numerical models have been identified in the literature which can be useful for its optimization. The third chapter of this paper refers to the creation of the numerical model of the large-scale solar collector. Due to the complex phenomena that take place inside the collector and the large number of lobed orifices present on the absorbent metal plate, it was necessary to design different two numerical models.

The first numerical model created analyses the numerical modelling of the air flow through the lobed orifices and studies the flow through a part of the collectors' absorbent plate (4 lobed orifices). The output data of this model is the input data for the second model studied, so that the effect of the orifices on the phase change materials can be correctly transposed. The second study refers to the numerical modelling of the large-scale collector, respectively the study of the flow and both temperature and velocity distributions through a "slice" of the large solar collector. A simplified, experimentally validated numerical model was thus obtained. Simulating the solar collector to its real dimensions would involve a very long calculation time due to a very large number of mesh cells, a period of time that would be practically unfeasible for the completion of studies. The temperature and velocity fields thus obtained from the first study were therefore integrated into the numerical model of the solar collector with large PCM. After making the numerical model that analyses the air flow through the lobed orifices (absorbent plate) we continued with the modelling of the actual solar collector with integrated phase change materials. The velocity and temperature fields resulting from the first model (outlet at 10De), were input data for the new numerical model (inlet). The modelling of the entire solar collector would involve a complex spatial discretization, respectively a very large number of cells within the computing domain in order to accurately capture the phenomena that take place.

The numerical models created and experimentally validated, represent another original contribution of this work, in the literature not being identified similar models and no such studies focused on the implementation of phase change materials in large solar air collectors with lobed orifices. The numerical model developed will be further studied and developed within post-doctoral studies, the current mode being a simplified one useful in order to optimize the calculation time periods in transient regime. This model will used for the parametric studies that will

be performed in order to optimize the prototype of the solar collector with integrated phase change materials. Different types of phase change materials with different melting / solidification temperatures, different amounts of PCMs, different types of inertial materials, different airflows, different positions of the PCM obstacle inside the air cavity, different orifices will be studied in order to optimize the solar collector until the optimal solution is identified.

Moreover, studies have shown a slow discharge of the energy stored within the phase change materials, which is also reported in the literature. Future studies will focus on improving the thermal conductivity of rectangular aluminium containers with integrated phase change materials by mounting metal fins with a role in increasing the heat exchange surface. Other innovative methods of increasing heat transfer refer to the implementation of nanoparticles within phase change materials, which has given birth to a subject studied intensively in the last three years called the study of nano-enhanced phase change materials [35]. The literature highlights that using metal fins, metal particles or nano-particles, the efficiency of heat transfer and the speed of melting / solidification processes can be improved when integrating phase change materials in solar collectors [36-38]. Leong et al. [39] points out that the ideal properties of the inertial materials with integrated nanoparticles are: high thermal conductivity, high energy storage capacity, phase change temperature suitable for the studied application, small volume variations, low investment cost, high stability and low sub-cooling temperature. There are a number of nano-particles that can be implemented that use metal, metal oxides, metal foams, carbon nano-tubes, carbon nano-particles, graphene and graphite and current technologies can even produce very small nano-particles [39]. Graphene and graphite are among the best nanoparticles that can be integrated into phase change materials and can determine a 101.2% higher thermal conductivity for only 3% concentration [40]. Moreover, by using graphite nanoparticles in concentrations between 0 and 10%, the thermal conductivity can be improved by 540 to 1000%, but attention must be paid to storage capacity that can decrease [41]. Therefore, phase change materials with integrated nano-particles have the potential to further enhance the operating time of solar air collectors, such systems not being studied so far [36, 42, 43].

The main conclusion of the current study is that the implementation of phase change materials within solar systems is a future solution that can increase their degree of implementation in buildings by increasing their overall efficiency and the number of hours of operation. The widespread implementation of solar air collectors and phase change materials will gradually reduce investment costs and their payback period will be more and more attractive, becoming over time common solutions in building applications.

<u>References – selection</u>

- 1. Catalina, T., A. Bejan, C. Butacu, M.-T. Pasti, and e. al., *Case eficiente energetic de la teorie la practica. Casa solara EFdeN*, ed. M. ROM. 2015.
- 2. Navarro, L., A. de Gracia, S. Colclough, M. Browne, S.J. McCormack, P. Griffiths, and L.F. Cabeza, *Thermal energy storage in building integrated thermal systems: A review. Part 1. active storage systems.* Renewable Energy, 2016. **88**: p. 526-547.
- 3. Hengstberger, F., C. Zauner, K. Resch, S. Holper, and M. Grobbauer, *High temperature phase change materials for the overheating protection of facade integrated solar thermal collectors.* Energy and Buildings, 2016. **124**: p. 1-6.
- 4. Heier, J., C. Bales, and V. Martin, *Combining thermal energy storage with buildings a review*. Renewable and Sustainable Energy Reviews, 2015. **42**: p. 1305-1325.
- 5. Australia's guide to environmentally sustainable homes. Australian Government, Department of Climate Change and Energy Efficiency. 2010.
- 6. Khadiran, T., M.Z. Hussein, Z. Zainal, and R. Rusli, *Advanced energy storage materials for building applications and their thermal performance characterization: A review.* Renewable and Sustainable Energy Reviews, 2016. 57: p. 916-928.
- 7. Soares, N., J.J. Costa, A.R. Gaspar, and P. Santos, Review of passive PCM latent heat thermal energy storage systems towards buildings' energy efficiency. Energy and Buildings, 2013. 59: p. 82-103.
- 8. Kylili, A. and P.A. Fokaides, *Life Cycle Assessment (LCA) of Phase Change Materials (PCMs) for building applications: A review.* Journal of Building Engineering, 2016. **6**: p. 133-143.
- 9. IEA. Solar's Untapped Potential. 2005; Available from: http://www.iea-shc.org/solarenergy/potential.htm.
- 10. Paya-Marin, M.A., Chapter 5 Solar Air Collectors for Cost-Effective Energy-Efficient Retrofitting, in Cost-Effective Energy Efficient Building Retrofitting. 2017, Woodhead Publishing. p. 141-168.
- 11. Shukla, A., D.N. Nkwetta, Y.J. Cho, V. Stevenson, and P. Jones, *A state of art review on the performance of transpired solar collector*. Renewable and Sustainable Energy Reviews, 2012. **16**(6): p. 3975-3985.

- 12. Alkilani, M.M., K. Sopian, M.A. Alghoul, M. Sohif, and M.H. Ruslan, *Review of solar air collectors with thermal storage units*. Renewable and Sustainable Energy Reviews, 2011. **15**(3): p. 1476-1490.
- 13. Rubitherm. [cited 2017]; Available from: https://www.rubitherm.eu/en/productCategories.html.
- 14. Poole, M.R., S.B. Shah, M.D. Boyette, L.F. Stikeleather, and T. Cleveland, *Performance of a coupled transpired solar collector—phase change material-based thermal energy storage system.* Energy and Buildings, 2018. **161**: p. 72-79.
- 15. Bejan, A.S., T. Catalina, and A.T. Munteanu, *Indoor Environmental Quality Experimental Studies in an Energy-efficient Building. Case study: EFdeN Project.* Energy Procedia, 2017. **112**: p. 269-276.
- 16. Entrop, A.G., H.J.H. Brouwers, and A.H.M.E. Reinders, Experimental research on the use of micro-encapsulated Phase Change Materials to store solar energy in concrete floors and to save energy in Dutch houses. Solar Energy, 2011. 85(5): p. 1007-1020.
- 17. Kuznik, F. and J. Virgone, Experimental assessment of a phase change material for wall building use. Applied Energy, 2009. **86**(10): p. 2038-2046.
- 18. Kuznik, F., J. Virgone, and J.-J. Roux, *Energetic efficiency of room wall containing PCM wallboard: A full-scale experimental investigation*. Energy and Buildings, 2008. **40**(2): p. 148-156.
- 19. Navarro, L., A. de Gracia, A. Castell, and L.F. Cabeza, *Experimental evaluation of a concrete core slab with phase change materials for cooling purposes*. Energy and Buildings, 2016. **116**: p. 411-419.
- 20. Navarro, L., A.d. Gracia, A. Castell, and L.F. Cabeza, *Experimental study of an active slab with PCM coupled to a solar air collector for heating purposes*. Energy and Buildings, 2016. **128**: p. 12-21.
- 21. Silva, T., R. Vicente, N. Soares, and V. Ferreira, Experimental testing and numerical modelling of masonry wall solution with PCM incorporation: A passive construction solution. Energy and Buildings, 2012. 49: p. 235-245.
- 22. Soares, N., A.R. Gaspar, P. Santos, and J.J. Costa, Experimental study of the heat transfer through a vertical stack of rectangular cavities filled with phase change materials. Applied Energy, 2015. 142: p. 192-205.
- 23. Soares, N., A.R. Gaspar, P. Santos, and J.J. Costa, Experimental evaluation of the heat transfer through small PCM-based thermal energy storage units for building applications. Energy and Buildings, 2016. 116: p. 18-34.
- 24. Dutil, Y., D. Rousse, S. Lassue, L. Zalewski, A. Joulin, J. Virgone, F. Kuznik, K. Johannes, J.-P. Dumas, J.-P. Bédécarrats, A. Castell, and L.F. Cabeza, *Modeling phase change materials behavior in building applications: Comments on material characterization and model validation.* Renewable Energy, 2014. **61**: p. 132-135.
- 25. Sharma, A., V.V. Tyagi, C.R. Chen, and D. Buddhi, *Review on thermal energy storage with phase change materials and applications*. Renewable and Sustainable Energy Reviews, 2009. **13**(2): p. 318-345.
- 26. Croitoru, C., I. Nastase, I. Voicu, A. Meslem, and M. Sandu, *Thermal Evaluation of an Innovative Type of Unglazed Solar Collector for Air Preheating*. Energy Procedia, 2016. **85**: p. 149-155.
- 27. Croitoru, C., I. Nastase, F. Bode, and A. Meslem, *Thermodynamic investigation on an innovative unglazed transpired solar collector*. Solar Energy, 2016. **131**: p. 21-29.
- 28. ANSYS, Manual Ansys Fluent Chapter 4.1.5. The k-omega and SST Models.
- 29. Ji, Y., CFD modelling of natural convection in air cavities. CFD Letters, 2014. Vol. 6 (1).
- 30. Croitoru, C. and I. Colda, Studii teoretice si experimentale referitoare la influenta turbulentei aerului din incaperile climatizate asupra confortului termic. 2011.
- 31. Bruno, F., USING PHASE CHANGE MATERIALS (PCMs) FOR SPACE HEATING AND COOLING IN BUILDINGS, in AIRAH performance enhanced buildings environmentally sustainable design conference. 2005.
- 32. Nkwetta, D.N. and F. Haghighat, *Thermal energy storage with phase change material—A state-of-the art review.* Sustainable Cities and Society, 2014. **10**: p. 87-100.
- 33. Tyagi, V.V. and D. Buddhi, *PCM thermal storage in buildings: A state of art.* Renewable and Sustainable Energy Reviews, 2007. **11**(6): p. 1146-1166.
- 34. Zhang, T., Y. Tan, H. Yang, and X. Zhang, *The application of air layers in building envelopes: A review.* Applied Energy, 2016. **165**: p. 707-734.
- 35. Ma, Z., W. Lin, and M.I. Sohel, *Nano-enhanced phase change materials for improved building performance*. Renewable and Sustainable Energy Reviews, 2016. **58**: p. 1256-1268.
- 36. Khan, M.M.A., N.I. Ibrahim, I.M. Mahbubul, H. Muhammad. Ali, R. Saidur, and F.A. Al-Sulaiman, *Evaluation of solar collector designs with integrated latent heat thermal energy storage: A review.* Solar Energy, 2018. **166**: p. 334-350.
- 37. Kasaeian, A., L. bahrami, F. Pourfayaz, E. Khodabandeh, and W.-M. Yan, Experimental studies on the applications of PCMs and nano-PCMs in buildings: A critical review. Energy and Buildings, 2017. 154: p. 96-112.
- 38. Li, W., D. Zhang, T. Jing, M. Gao, P. Liu, G. He, and F. Qin, *Nano-encapsulated phase change material slurry (Nano-PCMS)* saturated in metal foam: A new stable and efficient strategy for passive thermal management. Energy, 2018. **165**: p. 743-751.
- 39. Leong, K.Y., M.R. Abdul Rahman, and B.A. Gurunathan, *Nano-enhanced phase change materials: A review of thermo-physical properties, applications and challenges.* Journal of Energy Storage, 2019. **21**: p. 18-31.
- 40. Dsilva Winfred Rufuss, D., L. Suganthi, S. Iniyan, and P.A. Davies, *Effects of nanoparticle-enhanced phase change material* (NPCM) on solar still productivity. Journal of Cleaner Production, 2018. **192**: p. 9-29.
- 41. Zayed, M.E., J. Zhao, A.H. Elsheikh, Y. Du, F.A. Hammad, L. Ma, A.E. Kabeel, and S. Sadek, *Performance augmentation of flat plate solar water collector using phase change materials and nanocomposite phase change materials: A review.* Process Safety and Environmental Protection, 2019. **128**: p. 135-157.
- 42. Al-Jethelah, M., S.H. Tasnim, S. Mahmud, and A. Dutta, *Nano-PCM filled energy storage system for solar-thermal applications*. Renewable Energy, 2018. **126**: p. 137-155.
- 43. Qiu, L., Y. Ouyang, Y. Feng, and X. Zhang, *Review on micro/nano phase change materials for solar thermal applications*. Renewable Energy, 2019. **140**: p. 513-538.